Resource

Cell Chemical Biology

Integrative proximal-ubiquitomics profiling for deubiquitinase substrate discovery applied to USP30

Graphical abstract

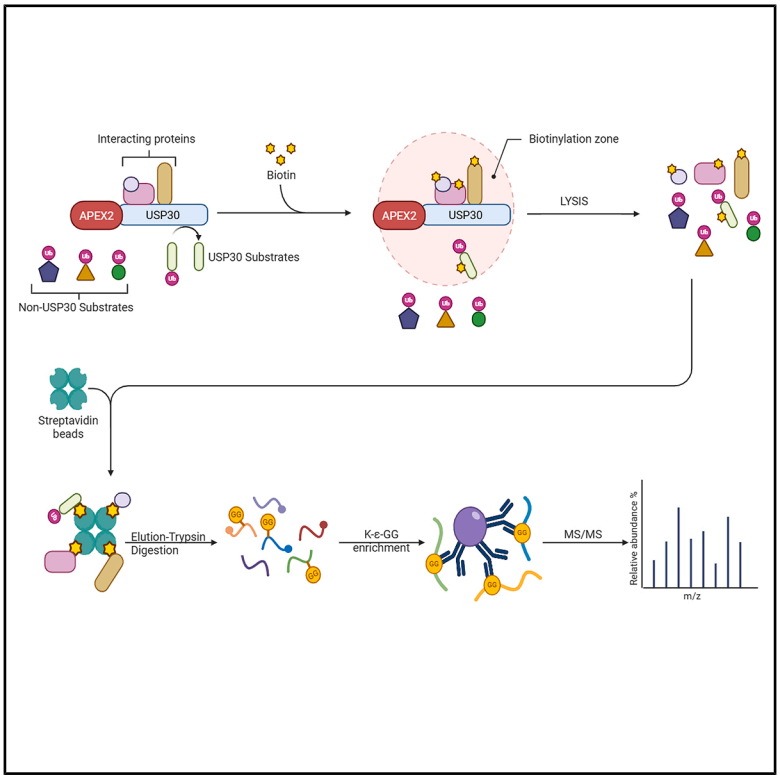

Authors

Andreas Damianou, Hannah B. L. Jones, Athina Grigoriou, ..., Iolanda Vendrell, Simon Davis, Benedikt M. Kessler

Correspondence

andreas.damianou@ndm.ox.ac.uk (A.D.), hannah.jones@ndm.ox.ac.uk (H.B.L.J.), benedikt.kessler@ndm.ox.ac.uk (B.M.K.)

In brief

Damianou et al. developed a technique to identify the protein targets of deubiquitinases. This approach allows researchers to investigate the specific locations and mechanisms of these enzymes within cells, offering an accurate method for elucidating their roles in regulating protein function and their potential as therapeutic targets.

Highlights

- APEX2 labeling can be integrated with K-ε-GG ubiquitin remnant enrichment
- This proximal-ubiquitome workflow facilitates the identification of DUB substrate
- Application of the approach captured the spatial ubiquitome of USP30 upon inhibition
- The method identified known (TOMM20, FKBP8) and additional (LETM1) substrates of USP30

Damianou et al., 2025, Cell Chemical Biology *32*, 1–16

https://doi.org/10.1016/j.chembiol.2025.04.004

CellPress

Please cite this article in press as: Damianou et al., Integrative proximal-ubiquitomics profiling for deubiquitinase substrate discovery applied to USP30, Cell Chemical Biology (2025), https://doi.org/10.1016/j.chembiol.2025.04.004

Cell Chemical Biology

CellPress
OPEN ACCESS

Resource

Integrative proximal-ubiquitomics profiling for deubiquitinase substrate discovery applied to USP30

Andreas Damianou,[1,2,5,*] Hannah B.L. Jones,[1,5,*] Athina Grigoriou,[1] Mohammed A. Akbor,[1] Edward Jenkins,[3] Philip D. Charles,[4] Iolanda Vendrell,[1,2] Simon Davis,[1,2] and Benedikt M. Kessler[1,2,6,*]

[1]Target Discovery Institute, Centre for Medicines Discovery, Nuffield Department of Medicine, University of Oxford, Roosevelt Drive, OX3 7FZ Oxford, UK

[2]Chinese Academy for Medical Sciences Oxford Institute, Nuffield Department of Medicine, University of Oxford, Roosevelt Drive, OX3 7FZ Oxford, UK

[3]Kennedy Institute of Rheumatology, University of Oxford, OX3 7FY Oxford, UK

[4]Big Data Institute, Nuffield Department of Medicine, University of Oxford, Oxford, UK

[5]These authors contributed equally

[6]Lead contact

*Correspondence: andreas.damianou@ndm.ox.ac.uk (A.D.), hannah.jones@ndm.ox.ac.uk (H.B.L.J.), benedikt.kessler@ndm.ox.ac.uk (B.M.K.)

https://doi.org/10.1016/j.chembiol.2025.04.004

SIGNIFICANCE Identifying direct substrates of deubiquitinases (DUBs) remains a significant challenge in the field of ubiquitin biology. In this study, we combine APEX2-based proximity labeling with enrichment of ubiquitin remnant motifs (K-ε-GG) to define candidate substrates within the native microenvironment of a DUB. This approach allows for the spatially resolved detection of site-specific deubiquitination events. When applied to the therapeutic target USP30, a mitochondrial DUB involved in mitophagy, the method successfully recovered several known substrates and identified LETM1 as a substrate. This strategy offers a robust framework for mapping DUB-substrate relationships and enhancing our understanding of ubiquitin-regulated pathways.

SUMMARY

The growing interest in deubiquitinases (DUBs) as drug targets for modulating critical molecular pathways in disease is fueled by the discovery of their specific cellular roles. A crucial aspect of this fact is the identification of DUB substrates. While mass spectrometry-based proteomic methods can be used to study global changes in cellular ubiquitination following DUB activity perturbation, these datasets often include indirect and downstream ubiquitination events. To enrich for the direct substrates of DUB enzymes, we have developed a proximal-ubiquitome workflow that combines proximity labeling methodology (ascorbate peroxidase-2 [APEX2]) with subsequent ubiquitination enrichment based on the K-ε-GG motif. We applied this technology to identify altered ubiquitination events in the vicinity of the DUB ubiquitin-specific protease 30 (USP30) upon its inhibition. Our findings reveal ubiquitination events previously associated with USP30 on TOMM20 and FKBP8, as well as the candidate substrate LETM1, which is deubiquitinated in a USP30-dependent manner.

INTRODUCTION

Ubiquitin (Ub) constitutes a highly conserved protein found across all eukaryotic organisms.[1] Ub can be activated and covalently attached to a target protein via the successive action of E1, E2, and E3 enzymes, forming a cascade that culminates in a post-translational modification. This intricate process plays an instrumental role in a myriad of cellular functions, encompassing protein homeostasis, signal transduction, DNA replication, and transcriptional regulation.[2]

E3 ligases and deubiquitinating proteases (DUBs) are specialist enzymes that add and remove covalent Ub modifications to and from target substrates. Both enzyme families are essential in the maintenance of Ub homeostasis. This dynamic

Please cite this article in press as: Damianou et al., Integrative proximal-ubiquitomics profiling for deubiquitinase substrate discovery applied to USP30, Cell Chemical Biology (2025), https://doi.org/10.1016/j.chembiol.2025.04.004

balance is integral to normal cellular operation and can alter the fate of Ub-modified proteins.[3] Imbalances in the ubiquitination of proteins have been implicated in various pathological conditions, including cancer and neurodegenerative diseases.[4,5] Therefore, the identification of E3 ligase/DUB substrates not only enriches our understanding of their biological roles but also opens avenues for the exploration of these enzymes as potential therapeutic targets.[6]

Several methodologies have been previously employed to identify potential substrates of E3 ligases. One category involves fusion techniques, such as UBAITS,[7] TULIP,[8] and TULIP2,[9] which use overexpressed Ub-E3 ligase fusions to trap and purify ligase-substrate adducts, often under denaturing conditions. These methodologies have pitfalls, including potential steric hinderance of the ubiquitin, and potential degradation of the E3 due to the conjugated Ub. Another category includes *in vitro* techniques such as E2-dID, orthogonal Ub transfer,[10,11] and microarray assays, which employ engineered enzymes or biotin-labeled Ub conjugates to target specific substrates.

Finally, UbPOD[12] and BioE3[13] are approaches that use tagged Ub as a biotinylation substrate for an E3 ligase conjugated to a proximity labeling enzyme. A drawback of these methods includes the overexpression of tagged ubiquitin, which may lead to altered ubiquitination events that are not physiologically relevant. Overall, while applicable to the formation of Ub-substrate bonds by E3s, these methodologies cannot be applied to study the breakage of these bonds by DUBs.

Here, we focus on developing a methodology to detect the substrates of DUBs, with site-specific deubiquitination information. Among the most established approaches to identify ubiquitination sites is the enrichment of the Ub remnant motif (K-ε-GG) left behind at the sites of lysine ubiquitination after protein trypsinization, followed by immunoprecipitation (IP) and subsequent mass spectrometry analysis.[14,15] The application of targeted knockouts, catalytically inactive mutants or of specific small-molecule inhibitors, in conjunction with the K-ε-GG technique can accelerate the identification process of DUB or E3 ligase substrates from specific alterations observed in the cellular ubiquitome.

However, the K-ε-GG method comes with limitations. One notable drawback is that many altered ubiquitination events may result from downstream secondary effects upon the reduced activity of a DUB or E3 ligase. While these events are of interest, they are not all reflective of direct enzyme substrates and activity. In the last decade, innovative proximity labeling approaches, such as BioID[16] and APEX,[17] have been developed to enhance the identification of proteins within the microenvironment of a protein of interest. Proximity labeling has previously been successfully integrated with phosphoenrichment strategies to investigate spatially referenced proximity phosphoproteomics.[18–20] In this study, we show that the effective combination of proximity labeling followed by post-translational modification enrichment can also be applied to the study of ubiquitination. This allows for the capture of protein ubiquitination states that are specifically localized to DUBs/E3 ligases. Application of the technique has the potential to enhance the resolution and accuracy of substrate identification of a DUB or E3 ligase upon the perturbation of its activity.

Ascorbate peroxidase-2 (APEX2) was considered favorable as a proximity labeling enzyme for this methodology due to the speed of the biotinylation reaction occurring on the second timescale. This labeling snapshot enables the capture of an acute cellular protein ubiquitination profile upon DUB inhibition/genetic depletion, without time-dependent convolution from the dynamic ubiquitination process. Additionally, APEX2 favors the biotinylation of tyrosine residues, meaning that it does not interfere with ubiquitination events occurring on lysine residues. Other proximity labeling approaches, such as BioID and TurboID, should not be applied to this methodology due to the long timescale of the labeling reaction and the biotinylation of lysine residues.

Ubiquitin-specific protease 30 (USP30) was selected as a model DUB for the development of this methodology due to its potential as a drug target, with the knockout of USP30 resulting in increased turnover of mitochondria via mitophagy.[21] The process of mitophagy could be targeted for multiple therapeutic applications, such as for the treatment of Parkinson's disease.[21,22] Therefore, further insights into the role USP30 plays in the process of mitophagy, and potential biomarkers resulting from its inhibition, are highly relevant. Additionally, previous characterization of the outer mitochondrial membrane (OMM) localization of USP30 and ubiquitomics studies of the activity of USP30 enable cross-validation of the proximal ubiquitome of USP30 to existing datasets.[22–24]

Here, we present the development of a workflow, combining APEX2 proximity labeling with subsequent K-ε-GG IP to elucidate the proximal ubiquitome of a target DUB (USP30), in both the presence and absence of an USP30 inhibitor, compound "**39**," a previously described potent, cell-permeable, and selective USP30 inhibitor.[25–27] The proximal-ubiquitomics methodology gives unique insight into the role of USP30 in the process of mitophagy. Potential direct USP30 substrates are uncovered through the application of the methodology, and subsequent validation provides evidence for USP30 enacting on the ubiquitination state of proteins considered critical to mitochondrial function and turnover. We focus on validating a previously undescribed potential USP30 substrate—leucine-containing zipper and EF-hand transmembrane protein 1 (LETM1), an essential protein described to be involved in mitochondrial ion transport, regulation of mitochondrial volume, energy metabolism, and maintenance of mitochondrial morphology.[28–31]

RESULTS

Proximal-ubiquitomic methodology optimization

Each aspect of the workflow applied in Figure 1 was optimized to ensure efficient capture of ubiquitinated proteins in the proximity of USP30 (Figure 2A). This is critical for the adaptation of the methodology to different systems. In this model USP30-APEX2 system, the conjugated enzymes were stably expressed in HEK293 cells with a low expression promoter (PGK).[32] We observed a moderate 3.8-fold increase in USP30 expression as compared to that of its endogenous expression levels (Figures 2B and S1A). Overexpression of USP30 has previously been demonstrated not to affect the levels of oxidative phosphorylation proteins[33] but can reduce the levels of mitophagy.[34] The overexpression of any DUB of interest conjugated to APEX2

Please cite this article in press as: Damianou et al., Integrative proximal-ubiquitomics profiling for deubiquitinase substrate discovery applied to USP30, Cell Chemical Biology (2025), https://doi.org/10.1016/j.chembiol.2025.04.004

CellPress
OPEN ACCESS

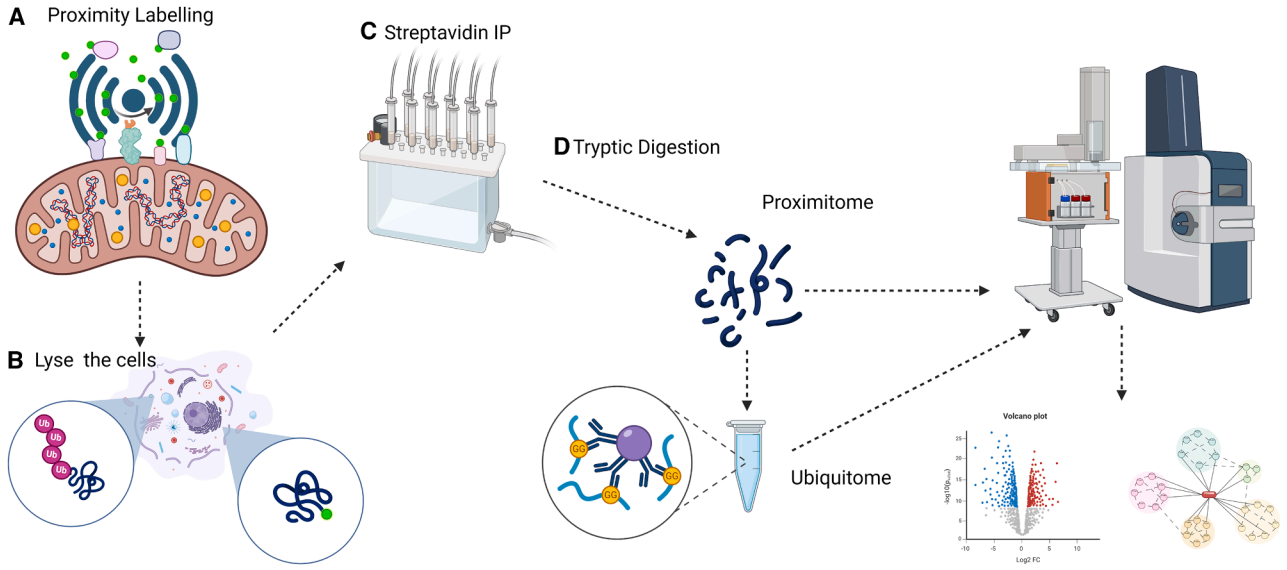

Figure 1. Integrated proximal-ubiquitomics methodology workflow

(A) Proximity labeling biotinylates the microenvironment of a DUB/E3 ligase of interest. (B) The cells are lysed. (C) The biotinylated proteins are then pulled down with streptavidin on the protein level to encompass ubiquitination events proximal to the biotinylation site. (D) Biotinylated proteins are then digested with trypsin, and ubiquitination events are enriched using a K-ε-GG antibody. Ubiquitinated proteins from the proximity of the enzyme of interest are then quantified by LC-MS/MS. Figure created using www.biorender.com.

may lead to different behavior of the enzyme, meaning it is important to use this methodology as a substrate discovery platform, with subsequent validations using endogenous levels of enzyme where possible.

Maintained USP30 activity was confirmed using a DUB activity-based probe (ABP), consisting of Ub with a propargylamine warhead and a hemagglutinin tag (HA-Ub-PA). The ~10 kDa molecular weight increase of USP30-APEX2 in the presence of HA-Ub-PA indicates that the active site of USP30 is still able to bind Ub and the active site cysteine is still reactive (Figures 2C and S1A). This ABP is broadly reactive with the majority of cysteine-active DUBs and so can be used to check retained activity if the proximal-ubiquitomics methodology is applied to other DUBs.[35] The maintained localization of USP30-APEX2 to the OMM was confirmed via TOMM20 co-localization microscopy (Figure 2D) and digitonin membrane isolation (Figure S1B).

After confirming that the properties of the DUB-APEX2 conjugate are reflective of the endogenous DUB, the APEX2 biotinylation labeling efficiency was optimized, to maximize the capture of proximal proteins. Incubating cells with a concentration range of biotin demonstrated that a minimum of 5 mM biotin was necessary for efficient protein biotinylation (Figure 2E). Treatment with biotin-phenol up to concentrations of 10 mM was not found to be cytotoxic (Figure S1C). In previous studies, biotin incubation with cells was performed for 30 min at 37°C with increased incubation not resulting in increased labeling, indicating that the incubation time is sufficient for full dispersal of biotin throughout the cells.[36] With the maximal biotinylation conditions, the volume of streptavidin beads then needs to be optimized to achieve efficient capture of all biotinylated proteins. By assessing the input, flow-through, and elution of the biotin streptavidin pull-down, we maximized the capture capacity of the streptavidin beads for this system with 1 mL of beads/10 mg of input protein (Figure 2F).

Once proteins proximal to USP30 were biotinylated by APEX2 and pulled down using streptavidin, the ubiquitination sites of these proteins were enriched for liquid chromatography-tandem mass spectrometry (LC-MS/MS) identification. This was achieved by trypsinizing the proteins and immunoprecipitating the K-ε-GG remnant motif that remains after the trypsinization of proteins reflecting ubiquitination, Neddylation, or ISGylation sites. However, under most normal physiological conditions, the source of most K-ε-GG remnant sites is ubiquitination (>94%).[37] Without K-ε-GG pull-down, we did not detect ubiquitination sites in the USP30 proximity labeling (data not shown), justifying the necessity for a subsequent enrichment step.

The recommended amount of protein material for K-ε-GG enrichment is 1–2 mg. Measurement of protein/peptide levels is challenging in the workflow due to interference from the presence of antioxidants in the lysis buffer. Additionally, proteins such as streptavidin and trypsin obscure the absolute protein quantitation after biotinylation elution and the peptide quantitation prior to the K-ε-GG enrichment, respectively. Therefore, material for this experimentation was optimized for the system based on the number of 15 cm plates at confluence used as starting material. When performing K-ε-GG enrichments without proximity enrichment, the number of identified K-ε-GG sites identified can vary greatly, depending on the source material, experimental conditions, and mass spectrometry methodology applied.[38,39]

In the case of the proximal-ubiquitomics workflow presented here, we saw a linear increase in the number of K-ε-GG sites with increasing input material, up to 4,000 sites with 10 × 15 cm plates (Figure 2G). However, the coverage of OMM-localized proteins that were identified as ubiquitinated

Please cite this article in press as: Damianou et al., Integrative proximal-ubiquitomics profiling for deubiquitinase substrate discovery applied to USP30, Cell Chemical Biology (2025), https://doi.org/10.1016/j.chembiol.2025.04.004

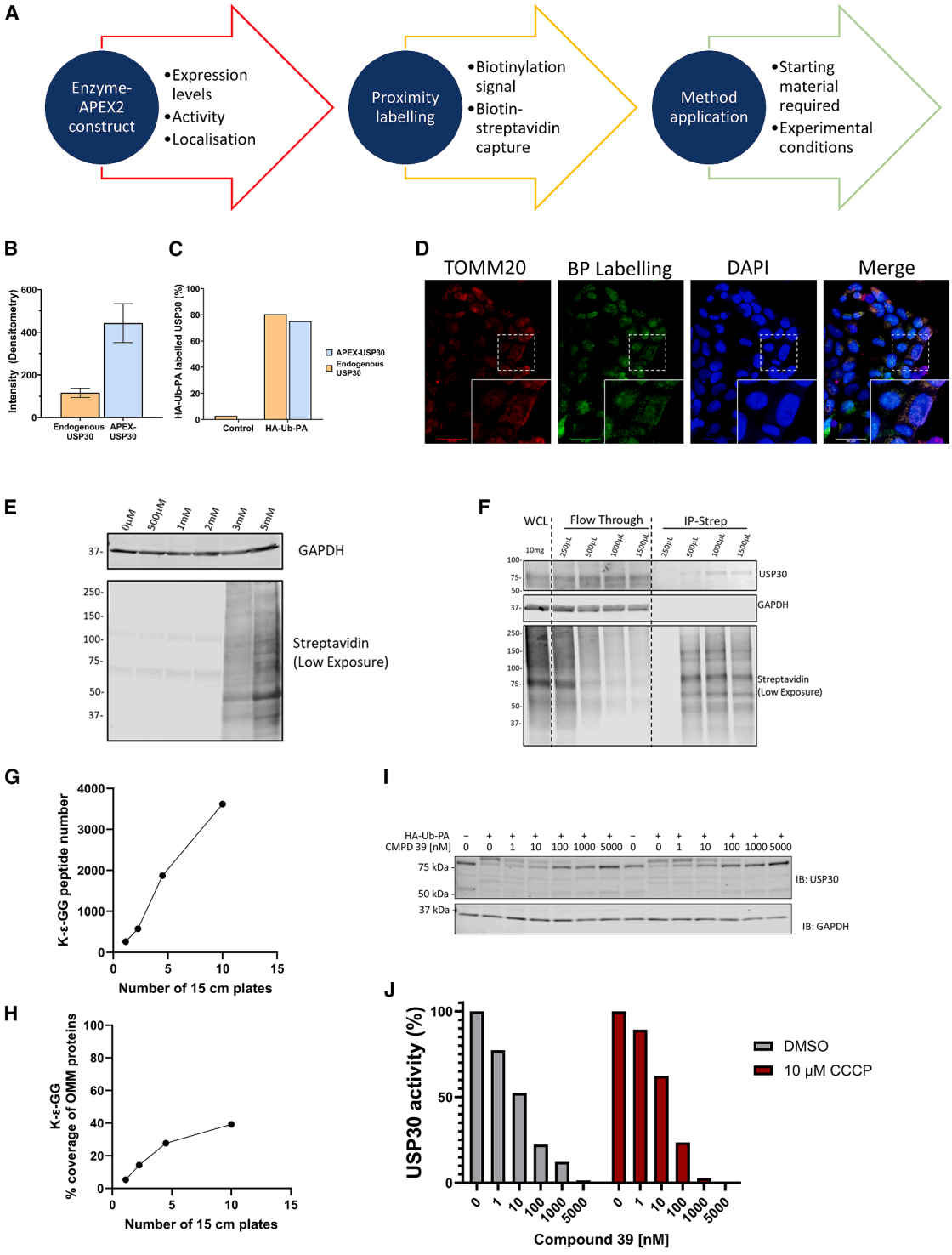

Figure 2. Optimization workflow for the proximal-ubiquitomics methodology

(A) Scheme of experimental optimization strategy.

(B) Densitometric intensity of HEK293 endogenous USP30 and APEX2-USP30 (n = 3 quantification of separate bands from 1 sample, error bars = SD).

(C) Percentage of endogenous and APEX2-conjugated USP30 labeled by HA-Ub-PA (n = 1).

(D) Immunofluorescence of TOMM20, biotin-phenol (BP), and DAPI staining after USP30-APEX2 biotinylation in HEK293 cells. Scale bars: 50 μm.

(E) Biotin-phenol concentration dependence of USP30-APEX2 biotinylation in HEK293 cells.

(F) Streptavidin pull-down optimization after USP30-APEX2 biotinylation with 5 mM biotin-phenol.

(G) Number of Gly-Gly peptides identified from the proximal-ubiquitomics methodology with different amounts of input material.

(legend continued on next page)

Please cite this article in press as: Damianou et al., Integrative proximal-ubiquitomics profiling for deubiquitinase substrate discovery applied to USP30, Cell Chemical Biology (2025), https://doi.org/10.1016/j.chembiol.2025.04.004

begins to plateau between 5 and 10 × 15 cm dishes of input material (Figure 2H). The increasing number of K-ε-GG sites not located on the OMM with increasing material input may be representative of an increasing background of proteins that are only infrequently and transiently within the USP30 microenvironment. Thus, 5 × 15 cm dishes per condition were selected as the optimal input material for this system to capture ubiquitination events proximal to USP30.

When applying this methodology to a different DUB and system, it is advised to use localization markers or known interactors as a cutoff for material input so as to enrich for proteins that consistently make up the microenvironment of a DUB. Where this information is unknown, a limiting amount of material should be used as input. The abundance of USP30 has been reported to be in the bottom 10% of ~8,000 proteins identified in a HEK293 proteome (PaxDB 5.0).[40,41] With the use of a low-expression promoter to mimic endogenous USP30 levels in this study, large amounts of input material were required for this model system. This may vary depending on expression levels of the protein of interest, and subsequently, the amount of material recovered post streptavidin IP.

After optimization of the USP30-APEX2 system and proximal-ubiquitomics workflow, experimental conditions to elucidate potential USP30 substrates using compound **39** (Figure S1E) were optimized. To maximize ubiquitination events in the proximity of USP30, cells were treated with carbonyl cyanide 3-chlorophenylhydrazone (CCCP) to depolarize the mitochondria and subsequently activate the PINK1/Parkin S65 phospho-ubiquitination pathway. Mitochondrial depolarization conditions have previously been shown to reveal increased OMM protein ubiquitination events as a consequence of USP30 knockout.[24] In this HEK293 USP30-APEX2 system, maximal S65 phospho-Ub was identified with 10 μM of CCCP cell treatment after 6 h of incubation (Figure S1D).

The concentration of the small-molecule compound **39** required for complete USP30 inhibition in the USP30-APEX2 overexpression system was assessed using the HA-Ub-PA ABP. After 6 h of cellular incubation, full inhibition of HA-Ub-PA binding to USP30-APEX2 was identified with 5 μM of compound **39**, regardless of the presence of 10 μM CCCP (Figures 2I and 2J). From this optimization, 10 μM CCCP treatment +/− 5 μM of compound **39** was applied to identify acute ubiquitination events proximal to USP30 occurring as a consequence of USP30 inhibition on mitochondria undergoing the process of mitophagy.

Optimized protocol reveals USP30 proximal ubiquitome enriched for OMM

The two conditions (CCCP treatment +/− 5 μM of compound **39**) were repeated in quadruplicate, with 5 × T175 flasks pooled per replicate. Although the method was optimized with 15 cm dishes, T175 flasks were implemented for this large experiment (surface area 145 cm^2 vs. 175 cm^2) to allow for the rapid removal of H_2O_2 and subsequent antioxidant washes by standing the flasks on end. The use of flasks rather than dishes can improve experimental efficiency where substantial input material is required. APEX2 biotin labeling was catalyzed by the addition of H_2O_2 and quenched with multiple antioxidant washes. After lysis, 5% of the material was taken for the "labeled proteome," with the remaining material used as input for the biotin-streptavidin pull-down. Equal input and eluate levels for each streptavidin pull-down were checked by western blot (Figure S1F). From this pull-down, 10% of eluates were taken for the "proximitome," and the remaining material was trypsinized and used as input for the K-ε-GG IP, forming the "proximal ubiquitome" (Figure 3A). Each step represents important information about the effect of USP30 inhibition as well as providing normalization data to ensure that ubiquitination events are not altered as a consequence of perturbed protein abundance or protein proximity to USP30 with compound **39** treatment.

To compare the method of the proxima -ubiquitome to the classical ubiquitomics workflow, we included a "labeled ubiquitome" (n = 3) with APEX2 biotinylation protein labeling, but without biotin enrichment by streptavidin. This allowed for the comparison of ubiquitination events occurring in the whole cell with those occurring in the proximity of USP30 in the same system. We also included a control proteome and ubiquitome (n = 4) without APEX2 biotinylation labeling ("normal proteome" and "normal ubiquitome"), to assess the effect of the biotin/H_2O_2 treatment and subsequent APEX2 biotinylation reaction on protein and ubiquitination site identification/quantification (Figure 3A). For reference, definitions of the experiment and experimental controls detailed in Figure 3A are outlined in Table 1.

The $\log_2$ intensities for all datasets averaged coefficients of variations (CVs) below 10%. The raw intensities showed higher CVs for the ubiquitomes compared to the proximitome/proteomes, with CVs for the proximal ubiquitome comparable to the control ubiquitomes (Figures S2A–S2F). Principal component analysis showed clustering of replicates based on the presence or absence of USP30 inhibition (Figures S2G–S2I).

To examine the effect of APEX2 biotin labeling on the proteome and ubiquitome of USP30-APEX2-expressing HEK293 cells, the labeled proteome was compared to the normal proteome, and the labeled ubiquitome was compared to the normal ubiquitome. There were significant changes to the intensity of proteins identified in the proteomes (Figure S3A), with String analysis[42] identifying that the majority of proteins with significantly increased intensities upon APEX2 labeling are structural constituents of chromatin (Figure S3B). This may be attributable to protein upregulation in response to DNA damage caused by the H_2O_2 treatment[43] during APEX2 labeling. No Mitocarta 3.0[44]-annotated proteins were altered, indicating that the labeling of proteins with biotin does not affect the detection and

(H) Percentage of outer mitochondrial membrane (OMM) Mitocarta 3.0 proteins identified from the proximal-ubiquitomics methodology with different amounts of input material.

(I) HA-Ub-PA-labeled USP30-APEX after a 6 h incubation of the USP30-APEX2 HEK293 cells with the indicated concentration of compound **39**, with and without 10 μM CCCP.

(J) Normalized densitometric quantification of USP30-APEX2 HA-Ub-PA labeling and inhibition after a 6 h incubation of the USP30-APEX2 HEK293 cells with the indicated concentration of compound **39**, with and without 10 μM CCCP (n = 1).

Please cite this article in press as: Damianou et al., Integrative proximal-ubiquitomics profiling for deubiquitinase substrate discovery applied to USP30, Cell Chemical Biology (2025), https://doi.org/10.1016/j.chembiol.2025.04.004

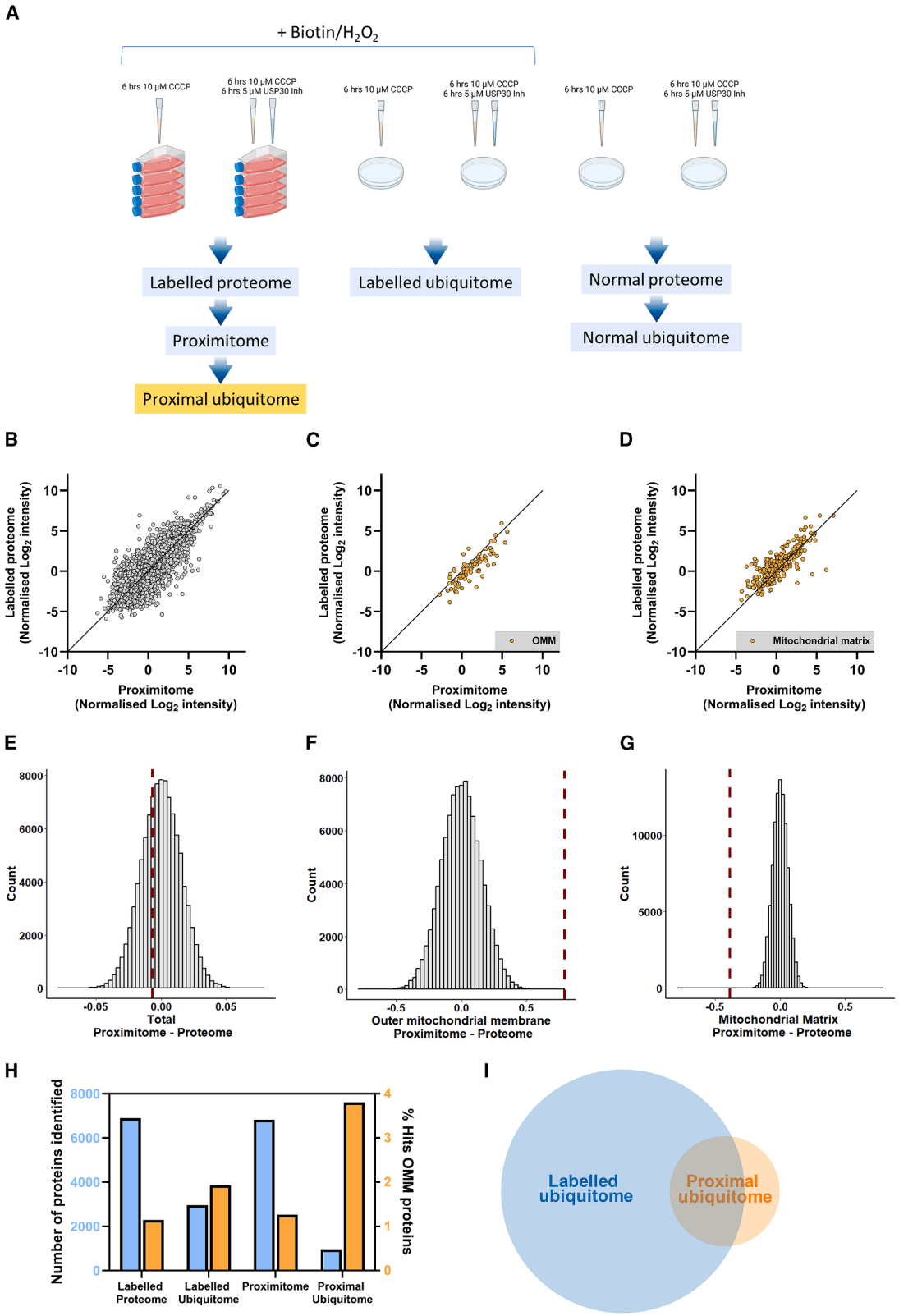

Figure 3. USP30 proximal ubiquitome enriched for outer mitochondrial membrane proteins

(A) Experimental design to compare the proximal ubiquitome of USP30 +/− compound **39,** with its corresponding proximitome, proteome, and ubiquitome. A control proteome and ubiquitome without APEX2 biotin labeling were also included for comparison.

(legend continued on next page)

Please cite this article in press as: Damianou et al., Integrative proximal-ubiquitomics profiling for deubiquitinase substrate discovery applied to USP30, Cell Chemical Biology (2025), https://doi.org/10.1016/j.chembiol.2025.04.004

intensity of the proteins anticipated to be proximal to USP30. There were also significant changes to the intensity of K-ε-GG peptides identified in the labeled ubiquitome when compared to the normal ubiquitome, including peptides originating from Mitocarta 3.0-annotated proteins (Figure S3C). The altered ubiquitome as a consequence of APEX2-catalyzed H_2O_2 biotin labeling is a limitation of proximity labeling and highlights the importance of subsequent validation of hits identified with proximal-ubiquitomics in systems lacking the APEX2 biotinylation process.

Proximity labelling of USP30-APEX2 has a high background due to its exposure to a vast number of cytoplasmic proteins and the large number of proteins that bind as background during the streptavidin pull-down. However, proteins that are most frequently proximal to USP30 will include genuine USP30 interactors, and therefore potential substrates of USP30. OMM proteins are a key example of this, with the fixed positioning of these proteins likely to increase their USP30-APEX2 biotinylation frequency and, consequently, their LC-MS/MS intensities. Additionally, previously identified USP30-dependent ubiquitination events are localized to the OMM, such as TOMM20.[21,22,24,45] To ensure the successful enrichment of proteins proximal to USP30-APEX2, the intensity of proteins annotated in Mitocarta 3.0 as OMM vs. mitochondrial matrix (MM) proteins was compared in the labeled proteome vs. the proximitome (Figures 3B–3D).

Permutation calculations were used to randomize the difference in X-Y scatter points in Figure 3B with the distribution of the average differences of the permutations plotted in Figure 3E. Here, the average difference in X-Y coordinates denoted by the red dashed line is within the normal distribution of the permutations, showing that the identified proteins are comparably intense between the proximitome and labeled proteome overall. When the same calculations are performed for the Mitocarta 3.0-annotated OMM proteins (Figures 3C and 3F) and MM proteins (Figures 3D and 3G), the average differences denoted by the red dashed line are significantly distinct from the randomized normal distribution, with the average difference never occurring in 100,000 permutations. These calculations show an enrichment of OMM proteins and a reduction of MM proteins in the proximitome when compared to the labeled proteome. Enrichment of OMM proteins in the proximitome vs. the labeled proteome was also determined by gene set enrichment analysis (GSEA) with other "mitoch" terms found to be diminished in the proximitome when compared to the labeled proteome (Figure S4). This confirms that the proximitome represents an enrichment of proteins that are situated within the proximity of USP30.

The enrichment of OMM proteins in the proximitome of USP30-APEX2 also translates to the proximal ubiquitome of the protein. The percentage of proteins linked to the OMM based on Mitocarta 3.0 annotation is doubled in the proximal ubiquitome compared to the control labeled ubiquitome (Figure 3H). Despite a reduced number of K-ε-GG-modified peptides identified in the proximal ubiquitome compared to the labeled ubiquitome, over 30% of proximal-ubiquitome peptides were not identified in the labeled ubiquitome (Figure 3I). This indicates that proximal-ubiquitomics in this system enriches for a subset of ubiquitination events from the proximity of USP30, thus narrowing down potential substrates of the DUB.

Application of proximal-ubiquitomics to uncover substrates of USP30

Following the experimental outline in Figure 3A, the labeled proteome and the proximitome were assessed for protein intensity alterations occurring as a consequence of USP30 inhibition (Figures 4A and 4B). Although some proteins were significant in their alterations (denoted in orange), only 1 protein in the labeled proteome and no proteins in the proximitome were increased or decreased more than a $\log_2$ fold change >1 with USP30 inhibition. Minimal changes to the proteome as a consequence of USP30 inhibition or knockout have also been previously reported in the literature.[22,45]

While proteins identified in the labeled proteome and USP30 proximitome were not perturbed upon USP30 inhibition, significant alterations to ubiquitinated peptide intensities as a consequence of USP30 inhibition were observed in the labeled ubiquitome and proximal ubiquitome (Figures 4C and 4D). Significant increases in the intensity of ubiquitinated peptides with USP30 inhibition represent potential USP30 substrates. Here, significantly increased ubiquitination (>1 $\log_2$ difference) is detected at various sites on 32 different proteins across the labeled ubiquitome and proximal ubiquitome (Figures 4E and 4F). Although exact ubiquitination sites vary, of the 32 proteins, 5 overlap between this dataset and two previously reported datasets with significantly increased ubiquitination events in the case of USP30 knockout in depolarizing conditions.[22,24] Those hits include TOMM20, FKBP8, VDAC2, VDAC1, and CISD1, all of which are Mitocarta 3.0 annotated as OMM proteins. Of the 5 hits, 2 are detected as significantly increased with USP30 inhibition in the labeled ubiquitome out of 25 in total. All 5 are detected as significantly increased with USP30 inhibition in the proximal ubiquitome out of 12 proteins in total (Figure 4G), indicative of the ability of the proximal-ubiquitomics technique to detect robust alterations occurring as a consequence of a reduction in USP30 activity across different cell types and experimental conditions.

The total number of increased ubiquitination events as a consequence of USP30 inhibition is substantially reduced in the proximal ubiquitome when compared to the labeled ubiquitome. A greater proportion of increased ubiquitination events

(B–D) The averaged $\log_2$ intensity of proteins quantified in the proximitome vs. proteome (with APEX2 biotinylation and CCCP treatment) with Mitocarta 3.0-annotated OMM proteins or MM proteins in orange.
(E–G) Permutation analysis – the dotted red line denotes the average of the X-Y intensity differences between the proximitome and the proteome of all proteins, outer mitochondrial membrane (OMM) proteins and mitochondrial membrane (MM) proteins. The distribution shows the randomized averages of these values over 100,000 permutations.
(H) The number of proteins identified in the biotin-labeled proteome, labeled ubiquitome, proximitome, and proximal ubiquitome vs. the percentage of Mitocarta 3.0 OMM-annotated proteins. Number of proteins taken from all samples in total, after filtering based on valid values as detailed in the STAR Methods section.
(I) The overlap in K-ε-GG peptides identified in the labeled ubiquitome and proximal ubiquitome.

Please cite this article in press as: Damianou et al., Integrative proximal-ubiquitomics profiling for deubiquitinase substrate discovery applied to USP30, Cell Chemical Biology (2025), https://doi.org/10.1016/j.chembiol.2025.04.004

Table 1. Definitions of experimental conditions

Term	Definition: LC-MS/MS analysis of -	Reason for experiment
Normal proteome	a total proteome of USP30-APEX2-expressing HEK293 cells treated with 10 μM CCCP +/− compound **39**, without APEX2-catalyzed biotin labeling	to assess the effect of APEX2 biotinylation on the proteome
Labeled proteome	a total proteome of USP30-APEX2-expressing HEK293 cells treated with 10 μM CCCP +/− compound **39**, with APEX2-catalyzed biotin labeling	for normalization, to assess whether compound **39**-induced proximal-ubiquitome changes are also changed on the proteome level
Normal ubiquitome	a ubiquitinated protein enrichment (K-ε-GG) of USP30-APEX2-expressing HEK293 cells treated with 10 μM CCCP +/− compound **39**, without APEX2-catalyzed biotin labeling	to assess the effect of APEX2 biotinylation on the ubiquitome
Labeled ubiquitome	a ubiquitinated protein enrichment (K-ε-GG) of USP30-APEX2-expressing HEK293 cells treated with 10 μM CCCP +/− compound **39**, with APEX2-catalyzed biotin labeling	for comparison of compound **39**-induced changes between the standard ubiquitome workflow to the proximal ubiquitome workflow
Proximitome	a streptavidin enrichment of biotinylated proteins labeled by APEX2 conjugated to USP30 in USP30-APEX2-expressing HEK293 cells treated with 10 μM CCCP +/− compound **39**	for normalization, to assess whether compound **39**-induced proximal-ubiquitome changes are also changed on the proximitome level
Proximal ubiquitome	a streptavidin enrichment of biotinylated proteins labeled by APEX2 conjugated to USP30 followed by a ubiquitin enrichment (K-ε-GG) in USP30-APEX2-expressing HEK293 cells treated with 10 μM CCCP +/− compound **39**	the main experimental dataset containing compound **39**-induced changes in ubiquitination occurring in proximity to USP30

are OMM in the proximal ubiquitome when compared to the labeled ubiquitome, whereas a smaller proportion of ubiquitination events occur on proteins associated with other parts of the mitochondria (Figure 4H). This finding is reflective of the enrichment of OMM proteins in the proximitome relative to the proteome and demonstrates that the proximal-ubiquitomics methodology is enabling the detection of changes in ubiquitination events occurring in the proximity of USP30.

LETM1 is a USP30 interactor and substrate

The increase in ubiquitination of OMM proteins with USP30 inhibition in the proximal ubiquitome has also been previously reported with USP30 knockout.[24] However, the increased ubiquitination of the inner mitochondrial membrane (IMM) protein LETM1 as a consequence of reduced USP30 activity has not previously been reported. The increase in LETM1 ubiquitination with USP30 inhibition was identified in both the labeled ubiquitome and proximal ubiquitome, and so LETM1 was further investigated as a potential USP30 substrate.

Initially, we sought to validate the proximity of USP30 to LETM1 using antibody-based proximity ligation assays (PLAs), allowing for the detection of proteins within a 30–40 nm proximity via fluorescence. In the absence of a selective USP30 antibody suitable for immunofluorescence/IP, FLAG-USP30 was overexpressed, and PLA was performed both with and without CCCP. A strong PLA signal confirmed that endogenous LETM1 and FLAG-USP30 are in proximity regardless of the presence of CCCP (Figure 5A). USP30 has previously been found to co-immunoprecipitate with TOMM20,[45] and the increased ubiquitination of TOMM20 with USP30 knockout in ubiquitomic experiments has previously been validated by western blot.[22,24] Therefore, TOMM20 was included as a positive control in experiments investigating LETM1 as a substrate of USP30. Here, endogenous TOMM20 was also identified as proximal to exogenous FLAG-USP30 by PLA, indicating that the exogenous FLAG-USP30 was correctly located on the mitochondria and co-localized to the TOMM complex (Figure 5B).

To further explore and increase our confidence regarding the proximity of USP30 to LETM1, a co-localization experiment was performed. FLAG-USP30 was overexpressed, and co-localization with endogenous LETM1 was assessed. Endogenous LETM1 and FLAG-USP30 co-localized, supporting the possibility that these two proteins could be in the same protein complex in the presence of CCCP (Figure 5C). To strengthen the validity of our co-localization findings, we calculated Li's intensity correlation quotient to quantify the degree of correlation between LETM1 and USP30 signals, resulting in a value of 0.182, which is indicative of a positive correlation. The USP30-LETM1 localization in the presence of CCCP was further validated with co-immunoprecipitation (coIP) experiments, where the pull-down of exogenous FLAG-USP30 captured endogenous LETM1 and the pull-down of endogenous LETM1 captured exogenous FLAG-USP30 (Figures 5D and 5E).

Additionally, coIP successfully captured endogenous TOMM20 where endogenous LETM1 was pulled down (Figure 5F). These data collectively support that LETM1 and USP30 are not only proximal to each other but also physically interact, either directly or indirectly. The interaction between these two proteins suggests that LETM1 may be a substrate of USP30, although this does not confirm USP30's ability to modify LETM1's ubiquitination status.

To further investigate, HEK293 cells were transfected with HA-Ub for 24 h, treated with CCCP and MG132, and the ubiquitinated proteome was purified by HA pull-down in both the presence and absence of compound **39**. Upon the IP of HA-ubiquitin, LETM1 displayed increased high-molecular-weight laddering in the presence of compound **39**, suggesting increased LETM1 ubiquitination with USP30 inhibition (Figure 6A). This increased

Please cite this article in press as: Damianou et al., Integrative proximal-ubiquitomics profiling for deubiquitinase substrate discovery applied to USP30, Cell Chemical Biology (2025), https://doi.org/10.1016/j.chembiol.2025.04.004

CellPress
OPEN ACCESS

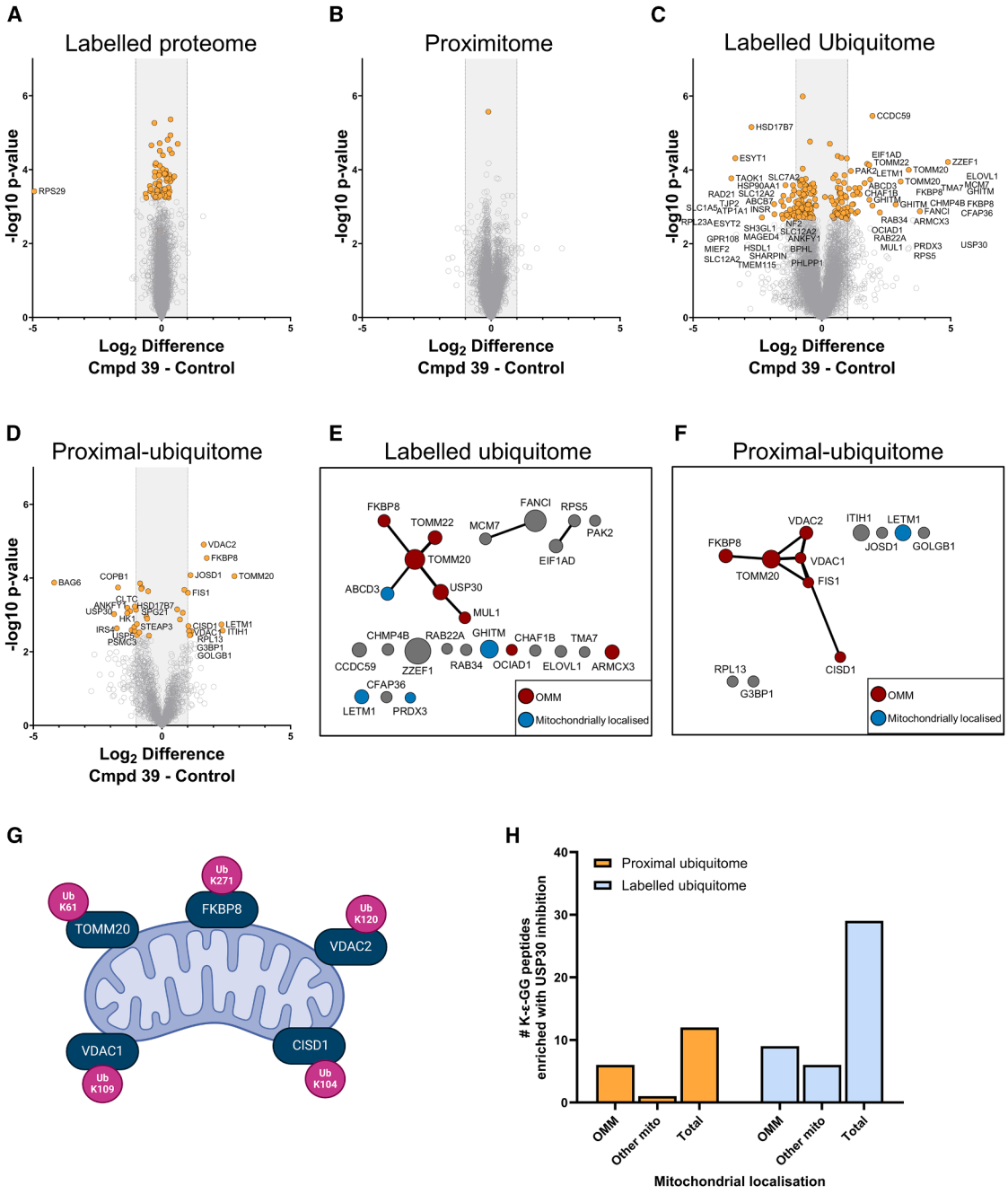

Figure 4. Discovery of USP30 substrate candidates by integrated proximal-ubiquitomics

(A) Labeled proteome volcano plot showing the effect of compound **39** treatment on protein levels in CCCP-treated HEK293 USP30-APEX2 cells with APEX2 biotin labeling.

(B) Proximitome volcano plot showing the effect of compound **39** treatment on protein levels captured from streptavidin pull-down after USP30-APEX2 biotinylation in CCCP-treated HEK293 USP30-APEX2 cells.

(C) Labeled ubiquitome volcano plot showing the effect of compound **39** treatment on peptides with K-ε-GG sites after K-ε-GG peptide enrichment in CCCP-treated HEK293 USP30-APEX2 cells with USP30-APEX2 biotin labeling.

(D) Proximal-ubiquitome volcano plot showing the effect of compound **39** treatment on peptides with K-ε-GG sites after streptavidin pull-down of USP30-APEX2 biotinylated proteins followed by K-ε-GG peptide enrichment in CCCP-treated HEK293 USP30-APEX2 cells. Volcano plot hits in orange = significant hits identified after permutation-based false discovery rate (FDR) correction at 5%.

(E and F) Cytoscape string analysis of K-ε-GG peptides that are significantly increased upon compound **39** treatment in CCCP-treated HEK293 USP30-APEX2 cells in the labeled ubiquitome (E) and proximal ubiquitome (F). Circle size is proportional to the $\log_2$ difference in K-ε-GG peptide intensity +/− compound **39** treatment, with the largest difference used if multiple peptides originate from the same protein. Red circles denote OMM, and blue circles denote other

(legend continued on next page)

Please cite this article in press as: Damianou et al., Integrative proximal-ubiquitomics profiling for deubiquitinase substrate discovery applied to USP30, Cell Chemical Biology (2025), https://doi.org/10.1016/j.chembiol.2025.04.004

laddering was also phenocopied with USP30 knockdown (Figure 6B).

To further validate this ubiquitination signal with an orthogonal technique, we also performed tandem ubiquitin-binding entity (TUBE) pull-downs on HEK293 cells treated with CCCP and +/− compound **39** (Figure 6C). Initially, we assessed the ubiquitination status of TOMM20 as a positive control, observing an accumulation of high-molecular-weight bands in the USP30-inhibited sample (Figure 6D). An increase in high-molecular-weight bands with TUBE enrichment was also seen with FKBP8 (Figure 6D), the ubiquitination of which has previously been reported to increase with USP30 knockout[22,24] but has not previously been validated.

Finally, upon USP30 inhibition, LETM1 exhibited high-molecular-weight laddering, indicating its increased ubiquitination in the TUBE-purified ubiquitinated proteome (Figure 6D). Taken together, altered LETM1 ubiquitination is arising as a direct consequence of USP30 activity and is not due to an enzyme scaffolding function or an off-target effect of the inhibitor.

A key function of LETM1 is in the regulation of mitochondrial morphology.[30,31] In order to investigate whether the increased ubiquitination of LETM1 as a consequence of USP30 knockdown led to a functional change in LETM1, we carried out lattice light-sheet microscopy of mitochondria. This approach enabled us to analyze tens of thousands of mitochondria across conditions providing robust statistics. Knockdown of USP30 using small interfering RNA (siRNA), however, only resulted in subtle shifts in mitochondria morphology, with a small increase in surface/volume ratio across the mitochondrial population, owing to changes predominantly in volume (Figure S5). This is in line with a previous report of USP30 activity affecting mitochondrial morphology subtly.[47]

DISCUSSION

Here, with USP30 as a model system, we have demonstrated that proximal-ubiquitomics enriches for events occurring in the proximity of the enzyme leading to a targeted list of positive ubiquitination hits for further validations. USP30 was selected as a model due to its status as a well-characterized DUB and the need to validate our methodology. This approach can be readily adapted to other DUBs of interest with minimal adjustments.

The optimization of the proximal-ubiquitome workflow presented here demonstrates the utility of combining the techniques of proximity labeling and ubiquitomic enrichment to elucidate direct substrates of a DUB in a cellular environment. Where protein ubiquitination "ubiquitomics" through the enrichment of the K-ε-GG Ub remnant motif can identify global alterations in the ubiquitomic state of proteins, it does not distinguish between direct and downstream ubiquitomic events occurring upon the perturbed activity of a DUB. The dynamic nature of ubiquitination events means that capturing and subsequently validating robust changes directly linked to an enzyme's activity can be challenging.

Proximity labeling is often employed to profile protein-protein interactions, including transient/weak interactions.[48] While proximity labeling offers a targeted insight into a protein's interactions and binding partners, here we demonstrate with APEX2 proximity labeling that the microenvironment of USP30 is not significantly altered upon inhibition of the enzyme. In this case, it may indicate that the enrichment of those proteins proximal to USP30 alone does not inform on substrates of the enzyme itself. Additionally, high background in proximity labeling experiments means that the proteins identified in the proximitome are not exclusively interactors of a protein of interest.[49] The power of applying proximity labeling alone rests where large changes in protein localization or complexes occur as a consequence of a stimulus.

Both ubiquitomic and proximity labeling studies have limitations for the identification of DUB substrates when applied alone, but, when combined together, they allow for the capture of ubiquitination events proximal to the enzyme of interest. By using ubiquitination as a readout, which changes when comparing an inhibited DUB to a non-inhibited version, or when comparing a wild-type protein to a catalytic-dead mutant, we gain insight into site-specific ubiquitination changes linked to the activity of a DUB. Additionally, by using APEX2 to label both strong and weakly interacting substrates in the local environment around our bait protein, we overcome the limitation of IP-based methods, which typically only capture strong interactions.

This was demonstrated by follow-up experiments exploring LETM1 as a potentially novel USP30 substrate. LETM1 is an IMM protein, which is essential[50] and is key to multiple mitochondrial functions such as the maintenance of mitochondrial morphology, mitochondrial tubular network assembly, and proton-dependent calcium efflux from mitochondria.[30,31,51–53]

Here, upon USP30 inhibition, LETM1 showed increased ubiquitination at K292, which is proposed to be located in the mitochondrial intermembrane space.[50,53] We were able to detect the co-localization of LETM1 with USP30 along with an altered ubiquitination state of LETM1 upon USP30 inhibition and knockdown. The interaction of USP30 with LETM1, despite their differential localization, may be originating from various cellular processes. One such process includes the proposed role of USP30 to deubiquitinate proteins that enter the mitochondria, with USP30 previously found to co-immunoprecipitate with the TOMM complex.[45] Here, we find that LETM1 also co-immunoprecipitates with TOMM20, indicating that the USP30-LETM1 interaction may occur upon mitochondrial import. However, this potential import role of USP30 may not be exactly clear as USP30 substrates are observed here to be predominantly located on the OMM, consistent with previous studies.[22]

mitochondrially localized Mitocarta 3.0-annotated proteins. Cytoscape String network based on string confidence score cutoff ≥0.7. Edge width is proportional to string confidence score.[42,46]

(G) K-ε-GG sites of the 5 proximal ubiquitome hits that overlap with altered ubiquitination states of proteins with USP30 inhibition/KO reported by Jones et al.[22] and Ordureau et al.[24]

(H) Number of K-ε-GG peptides with significantly increased intensity upon USP30 inhibition (significant hits from student's t test with permutation-based FDR correction at 5%, $\log_2$ difference >1) identified in the proximal ubiquitome and labeled ubiquitome either in total, with OMM localization, or with other mitochondrial localization annotation ("other mito") with Mitocarta 3.0 annotation.

Please cite this article in press as: Damianou et al., Integrative proximal-ubiquitomics profiling for deubiquitinase substrate discovery applied to USP30, Cell Chemical Biology (2025), https://doi.org/10.1016/j.chembiol.2025.04.004

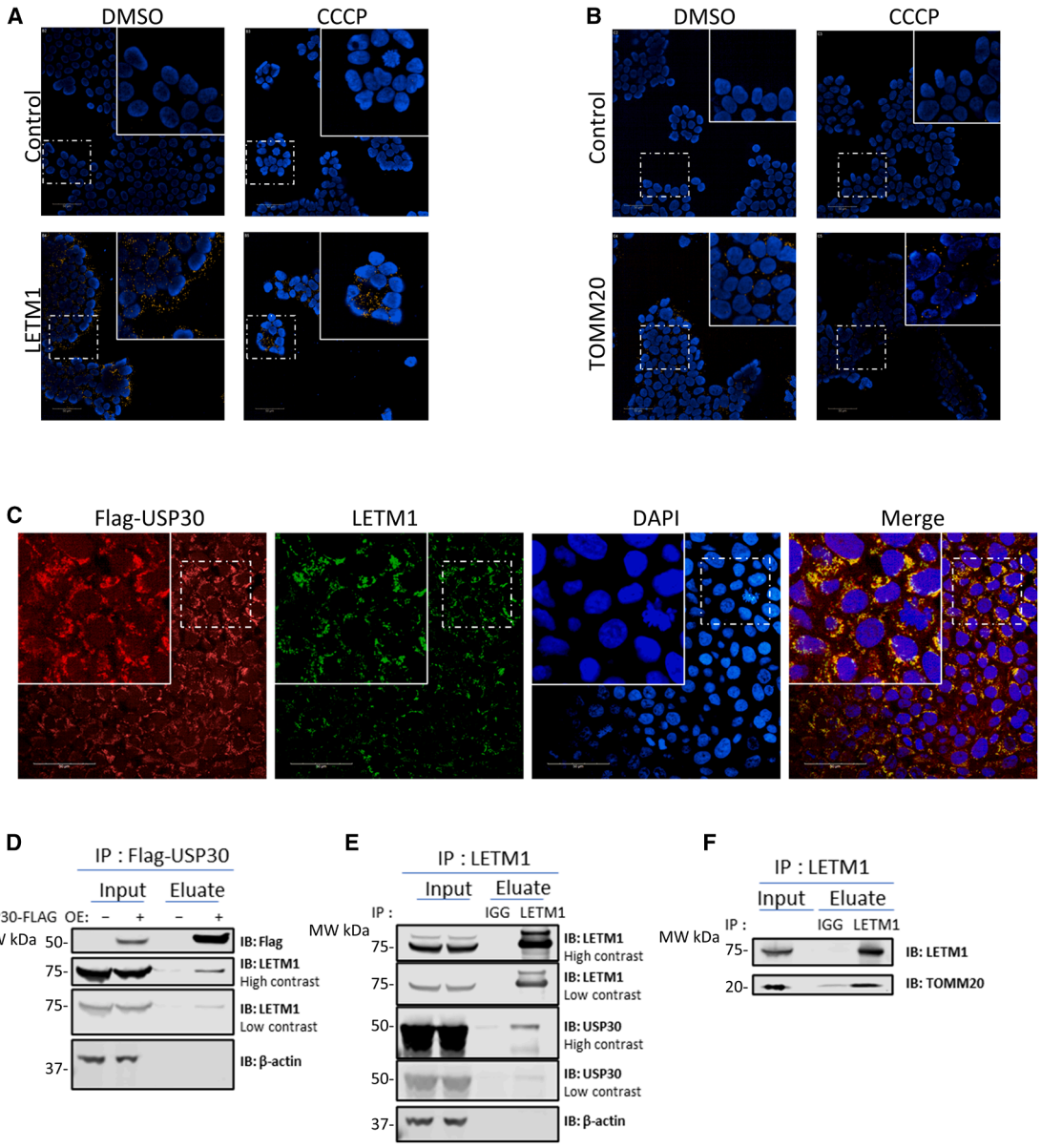

Figure 5. LETM1 as USP30 interactor

(A and B) Proximity ligation assay (PLA) in HEK293 cells. HEK293 cells transiently transfected with FLAG-USP30, with PLA reaction between anti-FLAG antibody and anti-LETM1 antibody (A) or an anti-TOMM20 antibody (B). Yellow punctate signals represent the reported interactions, and blue signals indicate nuclei. A single antibody control (none) was included. Scale bar: 50 μm.

(C) Confocal images of HEK293 cells +/− CCCP transiently expressing FLAG-USP30 and endogenous LETM1 protein. Anti-FLAG antibody (red), anti-LETM1 antibody (green), and DAPI (blue) for nuclei visualization. Scale bars: 10 μm.

(D and E) HEK293T cells transiently expressing FLAG-USP30 (D) USP30 was pulled down using an anti-FLAG antibody. (E) LETM1 was pulled down using an anti-LETM1 antibody.

(F) SH-SY5Y cell LETM1 pull-down using anti-LETM1 antibody.

Another possibility for USP30-LETM1 interactions includes minority mitochondrial outer membrane permeabilization, which has been found to occur with sublethal cellular stress.[54] Alternatively, LETM1 may interact with USP30 during vesicle formation of the IMM via herneation through the VDAC channels.[55] The increase in VDAC1 and VDAC2 ubiquitination upon reduction of USP30 activity seen both in this study as well as others indicates that USP30 may interact with VDAC proteins, and therefore may also be exposed to the IMM during this herneation process. Further experimentation is needed to fully characterize these processes in greater molecular detail.

As previously reported, LETM1 is known to play a role in mitochondrial morphology, so it was important to assess whether USP30 knockdown could lead to any morphological changes.

Please cite this article in press as: Damianou et al., Integrative proximal-ubiquitomics profiling for deubiquitinase substrate discovery applied to USP30, Cell Chemical Biology (2025), https://doi.org/10.1016/j.chembiol.2025.04.004

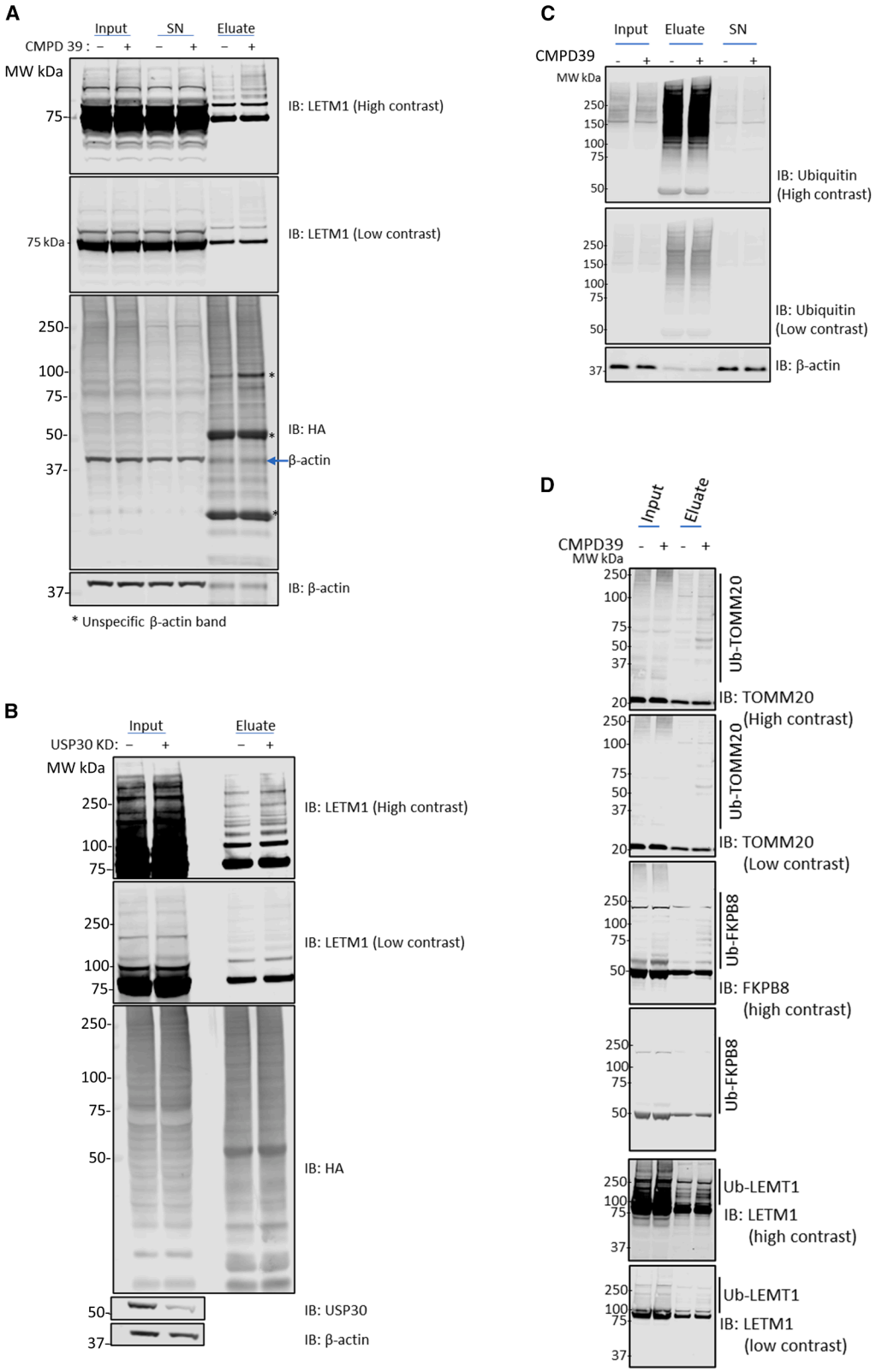

Figure 6. LETM1 and FKBP8 deubiquitination are USP30 dependent

(A) HA-ubiquitin pull-down using anti-HA antibody. HEK293T cells transiently expressing HA-Ub treated with 10 μM CCCP +/− compound **39**.

(B) HA-ubiquitin pull-down using anti-HA antibody. HEK293T cells transiently transfected with scrambled or USP30 siRNA and treated with 10 μM CCCP.

(C and D) Tandem ubiquitin binding entity (TUBE) pull-down in HEK293T cells treated with 10 μM CCCP +/− compound **39**.

Please cite this article in press as: Damianou et al., Integrative proximal-ubiquitomics profiling for deubiquitinase substrate discovery applied to USP30, Cell Chemical Biology (2025), https://doi.org/10.1016/j.chembiol.2025.04.004

Our data show a marginal increase in the mitochondrial surface-to-volume ratio, mainly due to changes in volume. This aligns with a previous report showing that USP30 activity affects mitochondrial morphology in a subtle way.[47] While this suggests that USP30 may have a role in shaping mitochondrial structure, at this stage, we have no evidence that this effect is LETM1 dependent. Whether USP30 influences mitochondrial morphology through LETM1 or through a different pathway remains an open question that will require further investigation.

The co-localization of USP30 to the TOMM complex was reproduced here with TOMM20-USP30 PLA and co-localization, as well as the previously validated increase in TOMM20 ubiquitination with reduced USP30 activity. We also confirmed increased ubiquitination of FKBP8 upon USP30 inhibition, which has been previously reported but not validated. The TOMM complex is critical for the import of mitochondrial preproteins,[56] and FKBP8 has been identified as a mitophagy receptor for Parkin-independent mitophagy.[57] The presence of LETM1, TOMM20, and FKBP8 in the proximal ubiquitome of USP30 increases the likelihood that they are direct USP30 substrates. Therefore, the proximal-ubiquitomics methodology developed here allows for an advanced insight into the action of the USP30 upon mitochondrial depolarization and how it may be influencing the mitophagy pathway.

The proximal-ubiquitomics approach builds upon previously described E3 ligase substrate detection methodologies, overcoming their limitations and allowing for the identification of specific ubiquitination events that could be applied as robust biomarkers of USP30 inhibition. More generally, proximal-ubiquitomics may be applicable more widely, not only for DUBs but also for E3 substrate discovery. The application of the methodology could guide the design of proteolysis-targeting chimeras (PROTACs), molecular glues, and deubiquitinase-targeting chimeras (DUBTACs) with translational potential.

Limitations of the study

A crucial consideration when applying this methodology to a new target is APEX2 labeling, which is highly dependent on the expression levels of the bait protein. Elevated DUB expression may lead to increased background signal, potentially affecting data quality. To mitigate this, we recommend using a promoter that drives moderate or low expression levels and rigorously validating APEX2 labeling through microscopy before proceeding with further analysis.

While LETM1 was identified as a potential USP30 substrate, the functional relevance of its deubiquitination by USP30, in the context of mitochondrial dynamics or metabolism, was not explored. USP30 is known to regulate mitophagy and mitochondrial homeostasis, and LETM1 has roles in mitochondrial ion exchange and morphology. However, their interplay remains to be functionally validated. All experiments were performed in HEK293 cells, which may not fully reflect the physiological context of USP30-LETM1 regulation.

RESOURCE AVAILABILITY

Lead contact

Further information and requests for resources and reagents should be directed to and will be fulfilled by the lead contact, Benedikt M. Kessler (benedikt.kessler@ndm.ox.ac.uk).

Materials availability

Plasmids generated in this study will be available from the lead contact upon request.

Data and code availability

- The mass spectrometry proteomics data have been deposited to the ProteomeXchange Consortium via the PRIDE[58] partner repository with the dataset identifier: PXD054890.
- Uncropped Western blot images have been uploaded to Mendeley Data: https://doi.org/10.17632/s7frkxwphg.1 and are publicly available.
- This study does not report any original code.
- Any additional information required to reanalyze the data reported in this paper is available from the lead contact upon request.

ACKNOWLEDGMENTS

We thank members of the Kessler and ODDI groups for helpful discussions. We also thank Val Miller and Daniel Ebner for using and guiding us with confocal microscopy. We would like to express our gratitude to Jesper Hansen for his guidance in analyzing the co-localization experiments. We thank Daryl S. Walter from Evotec for providing us with an aliquot of compound 39. H.B.L.J. was supported by a Bristol Myers Squibb fellowship. A.D., S.D., and B.M.K. were supported by the Chinese Academy of Medical Sciences (CAMS) Innovation Fund for Medical Science (CIFMS), China (grant number: 2018-I2M-2-002), and B.M.K. by the Engineering and Physical Sciences Research Council (EPSRC) grant (number: EP/N034295/1). E.J. was funded by Wellcome Trust (grant #224040/Z/21/Z). Imaging was performed using the Oxford-Zeiss Center of Excellent in Biomedical Imaging and the Kennedy Trust for Rheumatology Research (grant #202117 and 202103, respectively).

AUTHOR CONTRIBUTIONS

A.D. and H.B.L.J. contributed equally. A.D., H.B.L.J., and B.M.K. conceptualized the study. A.D., H.B.L.J., A.G., I.V., and S.D. conducted experiments. H.B.L.J., A.D., and P.D.C. analyzed data. B.M.K. supervised the experimental work. Funding was acquired by B.M.K. All authors wrote and approved the paper. M.A.A. performed GSEA analysis. E.J. performed lattice light-sheet microscopy of mitochondria.

DECLARATION OF INTERESTS

The authors declare no competing interests.

STAR★METHODS

Detailed methods are provided in the online version of this paper and include the following:

- KEY RESOURCES TABLE
- EXPERIMENTAL MODEL AND STUDY PARTICIPANT DETAILS
  - Cell culture
- METHOD DETAILS
  - Plasmid generation
  - Lentiviral packaging
  - Cell line generation
  - Transient transfection
  - Compound 39 synthesis
  - HA-Ub-PA ABP labelling
  - Membrane-cytoplasmic cellular fractionation
  - LDH release cytotoxicity assay
  - Proximal ubiquitomics workflow - APEX2 proximity labelling
  - Proximal ubiquitomics workflow - K-ε-GG immunoprecipitation
  - Control proteome, control ubiquitome and labelled ubiquitome
  - Liquid chromatography tandem mass spectrometry - LC-MS/MS
  - Immunofluorescence/Proximity ligation assay
  - Immunoprecipitation
  - Tandem ubiquitin binding entity pulldown

SUPPLEMENTAL INFORMATION

Supplemental information can be found online at https://doi.org/10.1016/j.chembiol.2025.04.004.

Received: October 17, 2024
Revised: March 7, 2025
Accepted: April 12, 2025
Published: May 5, 2025

REFERENCES

1. Zuin, A., Isasa, M., and Crosas, B. (2014). Ubiquitin Signaling: Extreme Conservation as a Source of Diversity. Cells *3*, 690–701. https://doi.org/10.3390/cells3030690.
2. Wilkinson, K.D. (1999). Ubiquitin-Dependent Signaling: The Role of Ubiquitination in the Response of Cells to Their Environment. J. Nutr. *129*, 1933–1936. https://doi.org/10.1093/jn/129.11.1933.
3. Reyes-Turcu, F.E., Ventii, K.H., and Wilkinson, K.D. (2009). Regulation and Cellular Roles of Ubiquitin-Specific Deubiquitinating Enzymes. Annu. Rev. Biochem. *78*, 363–397. https://doi.org/10.1146/annurev.biochem.78.082307.091526.
4. Deng, L., Meng, T., Chen, L., Wei, W., and Wang, P. (2020). The role of ubiquitination in tumorigenesis and targeted drug discovery. Signal Transduct. Target. Ther. *5*, 11. https://doi.org/10.1038/s41392-020-0107-0.
5. Le Guerroué, F., and Youle, R.J. (2021). Ubiquitin signaling in neurodegenerative diseases: an autophagy and proteasome perspective. Cell Death Differ. *28*, 439–454. https://doi.org/10.1038/s41418-020-00667-x.
6. Harrigan, J.A., Jacq, X., Martin, N.M., and Jackson, S.P. (2018). Deubiquitylating enzymes and drug discovery: emerging opportunities. Nat. Rev. Drug Discov. *17*, 57–78. https://doi.org/10.1038/nrd.2017.152.
7. O'Connor, H.F., Lyon, N., Leung, J.W., Agarwal, P., Swaim, C.D., Miller, K.M., and Huibregtse, J.M. (2015). Ubiquitin-Activated Interaction Traps (UBAITs) identify E3 ligase binding partners. EMBO Rep. *16*, 1699–1712. https://doi.org/10.15252/embr.201540620.
8. Kumar, R., González-Prieto, R., Xiao, Z., Verlaan-de Vries, M., and Vertegaal, A.C.O. (2017). The STUbL RNF4 regulates protein group SUMOylation by targeting the SUMO conjugation machinery. Nat. Commun. *8*, 1809. https://doi.org/10.1038/s41467-017-01900-x.
9. Salas-Lloret, D., Agabitini, G., and González-Prieto, R. (2019). TULIP2: An Improved Method for the Identification of Ubiquitin E3-Specific Targets. Front. Chem. *7*, 802. https://doi.org/10.3389/fchem.2019.00802.
10. Bhuripanyo, K., Wang, Y., Liu, X., Zhou, L., Liu, R., Duong, D., Zhao, B., Bi, Y., Zhou, H., Chen, G., et al. (2018). Identifying the substrate proteins of U-box E3s E4B and CHIP by orthogonal ubiquitin transfer. Sci. Adv. *4*, e1701393. https://doi.org/10.1126/sciadv.1701393.
11. Wang, Y., Liu, X., Zhou, L., Duong, D., Bhuripanyo, K., Zhao, B., Zhou, H., Liu, R., Bi, Y., Kiyokawa, H., and Yin, J. (2017). Identifying the ubiquitination targets of E6AP by orthogonal ubiquitin transfer. Nat. Commun. *8*, 2232. https://doi.org/10.1038/s41467-017-01974-7.
12. Mukhopadhyay, U., Levantovsky, S., Carusone, T.M., Gharbi, S., Stein, F., Behrends, C., and Bhogaraju, S. (2024). A ubiquitin-specific, proximity-based labeling approach for the identification of ubiquitin ligase substrates. Sci. Adv. *10*, eadp3000. https://doi.org/10.1126/sciadv.adp3000.
13. Barroso-Gomila, O., Merino-Cacho, L., Muratore, V., Perez, C., Taibi, V., Maspero, E., Azkargorta, M., Iloro, I., Trulsson, F., Vertegaal, A.C.O., et al. (2023). BioE3 identifies specific substrates of ubiquitin E3 ligases. Nat. Commun. *14*, 7656. https://doi.org/10.1038/s41467-023-43326-8.
14. Bustos, D., Bakalarski, C.E., Yang, Y., Peng, J., and Kirkpatrick, D.S. (2012). Characterizing Ubiquitination Sites by Peptide-based Immunoaffinity Enrichment. Mol. Cell. Proteomics *11*, 1529–1540. https://doi.org/10.1074/mcp.R112.019117.
15. Peng, J., Schwartz, D., Elias, J.E., Thoreen, C.C., Cheng, D., Marsischky, G., Roelofs, J., Finley, D., and Gygi, S.P. (2003). A proteomics approach to understanding protein ubiquitination. Nat. Biotechnol. *21*, 921–926. https://doi.org/10.1038/nbt849.
16. Roux, K.J., Kim, D.I., Raida, M., and Burke, B. (2012). A promiscuous biotin ligase fusion protein identifies proximal and interacting proteins in mammalian cells. J. Cell Biol. *196*, 801–810. https://doi.org/10.1083/jcb.201112098.
17. Lam, S.S., Martell, J.D., Kamer, K.J., Deerinck, T.J., Ellisman, M.H., Mootha, V.K., and Ting, A.Y. (2015). Directed evolution of APEX2 for electron microscopy and proximity labeling. Nat. Methods *12*, 51–54. https://doi.org/10.1038/nmeth.3179.
18. Huang, Y., Zhai, G., Fu, Y., Li, Y., Zang, Y., Lin, Y., and Zhang, K. (2024). A proximity labeling-based orthogonal trap strategy identifies HDAC8 promotes cell motility by modulating cortactin acetylation. Cell Chem. Biol. *31*, 514–522.e4. https://doi.org/10.1016/j.chembiol.2024.02.003.
19. Liu, Y., Zeng, R., Wang, R., Weng, Y., Wang, R., Zou, P., and Chen, P.R. (2021). Spatiotemporally resolved subcellular phosphoproteomics. Proc. Natl. Acad. Sci. USA *118*, e2025299118. https://doi.org/10.1073/pnas.2025299118.
20. Geoghegan, V., Carnielli, J.B.T., Jones, N.G., Saldivia, M., Antoniou, S., Hughes, C., Neish, R., Dowle, A., and Mottram, J.C. (2022). CLK1/CLK2-driven signalling at the Leishmania kinetochore is captured by spatially referenced proximity phosphoproteomics. Commun. Biol. *5*, 1305. https://doi.org/10.1038/s42003-022-04280-1.
21. Fang, T.-S.Z., Sun, Y., Pearce, A.C., Eleuteri, S., Kemp, M., Luckhurst, C.A., Williams, R., Mills, R., Almond, S., Burzynski, L., et al. (2023). Knockout or inhibition of USP30 protects dopaminergic neurons in a Parkinson's disease mouse model. Nat. Commun. *14*, 7295. https://doi.org/10.1038/s41467-023-42876-1.
22. Rusilowicz-Jones, E.V., Jardine, J., Kallinos, A., Pinto-Fernandez, A., Guenther, F., Giurrandino, M., Barone, F.G., McCarron, K., Burke, C.J., Murad, A., et al. (2020). USP30 sets a trigger threshold for PINK1–PARKIN amplification of mitochondrial ubiquitylation. Life Sci. Alliance *3*, e202000768. https://doi.org/10.26508/LSA.202000768.
23. Nakamura, N., and Hirose, S. (2008). Regulation of Mitochondrial Morphology by USP30, a Deubiquitinating Enzyme Present in the Mitochondrial Outer Membrane. Mol. Biol. Cell *19*, 1903–1911. https://doi.org/10.1091/mbc.e07-11-1103.
24. Ordureau, A., Paulo, J.A., Zhang, J., An, H., Swatek, K.N., Cannon, J.R., Wan, Q., Komander, D., and Harper, J.W. (2020). Global Landscape and Dynamics of Parkin and USP30-Dependent Ubiquitylomes in iNeurons during Mitophagic Signaling. Mol. Cell *77*, 1124–1142.e10. https://doi.org/10.1016/j.molcel.2019.11.013.
25. Rusilowicz-Jones, E.V., Barone, F.G., Lopes, F.M., Stephen, E., Mortiboys, H., Urbé, S., Urbé, U., and Clague, M.J. (2022). Benchmarking a highly selective USP30 inhibitor for enhancement of mitophagy and pexophagy. Life Sci. Alliance *5*, e202101287. https://doi.org/10.26508/LSA.202101287.
26. Jones, H.B.L., Heilig, R., Fischer, R., Kessler, B.M., and Pinto-Fernández, A. (2021). ABPP-HT - High-Throughput Activity-Based Profiling of Deubiquitylating Enzyme Inhibitors in a Cellular Context. Front. Chem. *9*, 44. https://doi.org/10.3389/FCHEM.2021.640105/BIBTEX.
27. O'Brien, D.P., Jones, H.B.L., Guenther, F., Murphy, E.J., England, K.S., Vendrell, I., Anderson, M., Brennan, P.E., Davis, J.B., Pinto-Fernández, A., et al. (2023). Structural Premise of Selective Deubiquitinase USP30

Inhibition by Small-Molecule Benzosulfonamides. Mol. Cell. Proteomics *22*, 100609. https://doi.org/10.1016/j.mcpro.2023.100609.

28. Shao, J., Fu, Z., Ji, Y., Guan, X., Guo, S., Ding, Z., Yang, X., Cong, Y., and Shen, Y. (2016). Leucine zipper-EF-hand containing transmembrane protein 1 (LETM1) forms a Ca2+/H+ antiporter. Sci. Rep. *6*, 34174. https://doi.org/10.1038/srep34174.
29. Piao, L., Li, Y., Kim, S.J., Sohn, K.-C., Yang, K.-J., Park, K.A., Byun, H.S., Won, M., Hong, J., Hur, G.M., et al. (2009). Regulation of OPA1-mediated mitochondrial fusion by leucine zipper/EF-hand-containing transmembrane protein-1 plays a role in apoptosis. Cell. Signal. *21*, 767–777. https://doi.org/10.1016/j.cellsig.2009.01.020.
30. Dimmer, K.S., Navoni, F., Casarin, A., Trevisson, E., Endele, S., Winterpacht, A., Salviati, L., and Scorrano, L. (2008). LETM1, deleted in Wolf Hirschhorn syndrome is required for normal mitochondrial morphology and cellular viability. Hum. Mol. Genet. *17*, 201–214. https://doi.org/10.1093/hmg/ddm297.
31. Tamai, S., Iida, H., Yokota, S., Sayano, T., Kiguchiya, S., Ishihara, N., Hayashi, J.-I., Mihara, K., and Oka, T. (2008). Characterization of the mitochondrial protein LETM1, which maintains the mitochondrial tubular shapes and interacts with the AAA-ATPase BCS1L. J. Cell Sci. *121*, 2588–2600. https://doi.org/10.1242/jcs.026625.
32. Qin, J.Y., Zhang, L., Clift, K.L., Hulur, I., Xiang, A.P., Ren, B.-Z., and Lahn, B.T. (2010). Systematic Comparison of Constitutive Promoters and the Doxycycline-Inducible Promoter. PLoS One *5*, e10611. https://doi.org/10.1371/journal.pone.0010611.
33. Tsefou, E., Walker, A.S., Clark, E.H., Hicks, A.R., Luft, C., Takeda, K., Watanabe, T., Ramazio, B., Staddon, J.M., Briston, T., and Ketteler, R. (2021). Investigation of USP30 inhibition to enhance Parkin-mediated mitophagy: tools and approaches. Biochem. J. *478*, 4099–4118. https://doi.org/10.1042/BCJ20210508.
34. Bingol, B., Tea, J.S., Phu, L., Reichelt, M., Bakalarski, C.E., Song, Q., Foreman, O., Kirkpatrick, D.S., and Sheng, M. (2014). The mitochondrial deubiquitinase USP30 opposes parkin-mediated mitophagy. Nature *510*, 370–375. https://doi.org/10.1038/nature13418.
35. Pinto-Fernández, A., Davis, S., Schofield, A.B., Scott, H.C., Zhang, P., Salah, E., Mathea, S., Charles, P.D., Damianou, A., Bond, G., et al. (2019). Comprehensive Landscape of Active Deubiquitinating Enzymes Profiled by Advanced Chemoproteomics. Front. Chem. *7*, 592. https://doi.org/10.3389/fchem.2019.00592.
36. Liang, Z., Damianou, A., Grigoriou, A., Jones, H.B.L., Sharlandijeva, V., Lassen, F., Vendrell, I., Di Daniel, E., and Kessler, B.M. (2024). Protocol to profile spatially resolved NLRP3 inflammasome complexes using APEX2-based proximity labeling. STAR Protoc. *5*, 103417. https://doi.org/10.1016/j.xpro.2024.103417.
37. Kim, W., Bennett, E.J., Huttlin, E.L., Guo, A., Li, J., Possemato, A., Sowa, M.E., Rad, R., Rush, J., Comb, M.J., et al. (2011). Systematic and quantitative assessment of the ubiquitin-modified proteome. Mol. Cell *44*, 325–340. https://doi.org/10.1016/J.MOLCEL.2011.08.025.
38. Vere, G., Kealy, R., Kessler, B.M., and Pinto-Fernandez, A. (2020). Ubiquitomics: An overview and future. Preprint at: MDPI AG. https://doi.org/10.3390/biom10101453
39. Steger, M., Demichev, V., Backman, M., Ohmayer, U., Ihmor, P., Müller, S., Ralser, M., and Daub, H. (2021). Time-resolved in vivo ubiquitinome profiling by DIA-MS reveals USP7 targets on a proteome-wide scale. Nat. Commun. *12*, 5399. https://doi.org/10.1038/s41467-021-25454-1.
40. Wang, M., Herrmann, C.J., Simonovic, M., Szklarczyk, D., and von Mering, C. (2015). Version 4.0 of PaxDb: Protein abundance data, integrated across model organisms, tissues, and cell-lines. Proteomics *15*, 3163–3168. https://doi.org/10.1002/pmic.201400441.
41. Geiger, T., Wehner, A., Schaab, C., Cox, J., and Mann, M. (2012). Comparative Proteomic Analysis of Eleven Common Cell Lines Reveals Ubiquitous but Varying Expression of Most Proteins. Mol. Cell. Proteomics *11*, M111.014050. https://doi.org/10.1074/mcp.M111.014050.
42. Szklarczyk, D., Kirsch, R., Koutrouli, M., Nastou, K., Mehryary, F., Hachilif, R., Gable, A.L., Fang, T., Doncheva, N.T., Pyysalo, S., et al. (2023). The STRING database in 2023: protein–protein association networks and functional enrichment analyses for any sequenced genome of interest. Nucleic Acids Res. *51*, D638–D646. https://doi.org/10.1093/nar/gkac1000.
43. Imlay, J.A., Chin, S.M., and Linn, S. (1988). Toxic DNA Damage by Hydrogen Peroxide Through the Fenton Reaction in Vivo and in Vitro. Science (1979) *240*, 640–642. https://doi.org/10.1126/science.2834821.
44. Rath, S., Sharma, R., Gupta, R., Ast, T., Chan, C., Durham, T.J., Goodman, R.P., Grabarek, Z., Haas, M.E., Hung, W.H.W., et al. (2021). MitoCarta3.0: an updated mitochondrial proteome now with sub-organelle localization and pathway annotations. Nucleic Acids Res. *49*, D1541–D1547. https://doi.org/10.1093/NAR/GKAA1011.
45. Phu, L., Rose, C.M., Tea, J.S., Wall, C.E., Verschueren, E., Cheung, T.K., Kirkpatrick, D.S., and Bingol, B. (2020). Dynamic Regulation of Mitochondrial Import by the Ubiquitin System. Mol. Cell *77*, 1107–1123. e10. https://doi.org/10.1016/j.molcel.2020.02.012.
46. Shannon, P., Markiel, A., Ozier, O., Baliga, N.S., Wang, J.T., Ramage, D., Amin, N., Schwikowski, B., and Ideker, T. (2003). Cytoscape: A Software Environment for Integrated Models of Biomolecular Interaction Networks. Genome Res. *13*, 2498–2504. https://doi.org/10.1101/gr.1239303.
47. Williamson, M.G., Heon-Roberts, R., Franks, S.N.J., Mock, E., Jones, H.B.L., Britti, E., Malpartida, A., Bassal, M., Lavelle, M., Connor, J., et al. (2025). USP30 Inhibition Improves Mitochondrial Health through Both PINK1-dependent and Independent Mechanisms. Preprint at: Cold Spring Harbor Laboratory. https://doi.org/10.1101/2025.02.03.636341
48. Bosch, J.A., Chen, C.L., and Perrimon, N. (2021). Proximity-dependent labeling methods for proteomic profiling in living cells: An update. WIREs Developmental Biology *10*, e392. https://doi.org/10.1002/wdev.392.
49. Damianou, A., Liang, Z., Lassen, F., Vendrell, I., Vere, G., Hester, S., Charles, P.D., Pinto-Fernandez, A., Santos, A., Fischer, R., and Kessler, B.M. (2024). Oncogenic mutations of KRAS modulate its turnover by the CUL3/LZTR1 E3 ligase complex. Life Sci. Alliance *7*, e202302245. https://doi.org/10.26508/lsa.202302245.
50. Austin, S., and Nowikovsky, K. (2019). LETM1: Essential for Mitochondrial Biology and Cation Homeostasis? Trends Biochem. Sci. *44*, 648–658. https://doi.org/10.1016/j.tibs.2019.04.002.
51. Jiang, D., Zhao, L., and Clapham, D.E. (2009). Genome-Wide RNAi Screen Identifies Letm1 as a Mitochondrial Ca^{2+}/H^{+} Antiporter. Science (1979) *326*, 144–147. https://doi.org/10.1126/science.1175145.
52. Tsai, M.-F., Jiang, D., Zhao, L., Clapham, D., and Miller, C. (2014). Functional reconstitution of the mitochondrial Ca2+/H+ antiporter Letm1. J. Gen. Physiol. *143*, 67–73. https://doi.org/10.1085/jgp.201311096.
53. Natarajan, G.K., Mishra, J., Camara, A.K.S., and Kwok, W.M. (2021). LETM1: A Single Entity With Diverse Impact on Mitochondrial Metabolism and Cellular Signaling. Front. Physiol. *12*, 637852. https://doi.org/10.3389/FPHYS.2021.637852/BIBTEX.
54. Ichim, G., Lopez, J., Ahmed, S.U., Muthalagu, N., Giampazolias, E., Delgado, M.E., Haller, M., Riley, J.S., Mason, S.M., Athineos, D., et al. (2015). Limited Mitochondrial Permeabilization Causes DNA Damage and Genomic Instability in the Absence of Cell Death. Mol. Cell *57*, 860–872. https://doi.org/10.1016/j.molcel.2015.01.018.
55. Prashar, A., Bussi, C., Fearns, A., Capurro, M.I., Gao, X., Sesaki, H., Gutierrez, M.G., and Jones, N.L. (2024). Lysosomes drive the piecemeal removal of mitochondrial inner membrane. Nature *632*, 1110–1117. https://doi.org/10.1038/s41586-024-07835-w.
56. Araiso, Y., Tsutsumi, A., Qiu, J., Imai, K., Shiota, T., Song, J., Lindau, C., Wenz, L.-S., Sakaue, H., Yunoki, K., et al. (2019). Structure of the mitochondrial import gate reveals distinct preprotein paths. Nature *575*, 395–401. https://doi.org/10.1038/s41586-019-1680-7.
57. Bhujabal, Z., Birgisdottir, Å.B., Sjøttem, E., Brenne, H.B., Øvervatn, A., Habisov, S., Kirkin, V., Lamark, T., and Johansen, T. (2017). FKBP8

recruits LC3A to mediate Parkin-independent mitophagy. EMBO Rep. *18*, 947–961. https://doi.org/10.15252/embr.201643147.

58. Perez-Riverol, Y., Bai, J., Bandla, C., García-Seisdedos, D., Hewapathirana, S., Kamatchinathan, S., Kundu, D.J., Prakash, A., Frericks-Zipper, A., Eisenacher, M., et al. (2022). The PRIDE database resources in 2022: a hub for mass spectrometry-based proteomics evidences. Nucleic Acids Res. *50*, D543–D552. https://doi.org/10.1093/nar/gkab1038.

59. Tyanova, S., Temu, T., Sinitcyn, P., Carlson, A., Hein, M.Y., Geiger, T., Mann, M., and Cox, J. (2016). The Perseus computational platform for comprehensive analysis of (prote)omics data. Nat. Methods *13*, 731–740. https://doi.org/10.1038/nmeth.3901.

60. Wu, T., Hu, E., Xu, S., Chen, M., Guo, P., Dai, Z., Feng, T., Zhou, L., Tang, W., Zhan, L., et al. (2021). clusterProfiler 4.0: A universal enrichment tool for interpreting omics data. Innovation *2*, 100141. https://doi.org/10.1016/j.xinn.2021.100141.

61. van der Walt, S., Schönberger, J.L., Nunez-Iglesias, J., Boulogne, F., Warner, J.D., Yager, N., Gouillart, E., and Yu, T.; scikit-image contributors (2014). scikit-image: image processing in Python. PeerJ *2*, e453. https://doi.org/10.7717/peerj.453.

62. Sowa, M.E., Bennett, E.J., Gygi, S.P., and Harper, J.W. (2009). Defining the Human Deubiquitinating Enzyme Interaction Landscape. Cell *138*, 389–403. https://doi.org/10.1016/j.cell.2009.04.042.

63. Liang, Z., Damianou, A., Vendrell, I., Jenkins, E., Lassen, F.H., Washer, S. J., Grigoriou, A., Liu, G., Yi, G., Lou, H., et al. (2024). Proximity proteomics reveals UCH-L1 as an essential regulator of NLRP3-mediated IL-1β production in human macrophages and microglia. Cell Rep. *43*, 114152. https://doi.org/10.1016/j.celrep.2024.114152.

64. Muntel, J., Kirkpatrick, J., Bruderer, R., Huang, T., Vitek, O., Ori, A., and Reiter, L. (2019). Comparison of Protein Quantification in a Complex Background by DIA and TMT Workflows with Fixed Instrument Time. J. Proteome Res. *18*, 1340–1351. https://doi.org/10.1021/ACS.JPROTEOME.8B00898/SUPPL_FILE/PR8B00898_SI_012.XLSX.

65. Meier, F., Brunner, A.-D., Frank, M., Ha, A., Bludau, I., Voytik, E., Kaspar-Schoenefeld, S., Lubeck, M., Raether, O., Bache, N., et al. (2020). diaPASEF: parallel accumulation–serial fragmentation combined with data-independent acquisition. Nat. Methods *17*, 1229–1236. https://doi.org/10.1038/s41592-020-00998-0.

66. Demichev, V., Messner, C.B., Vernardis, S.I., Lilley, K.S., and Ralser, M. (2020). DIA-NN: neural networks and interference correction enable deep proteome coverage in high throughput. Nat. Methods *17*, 41–44. https://doi.org/10.1038/s41592-019-0638-x.

67. R Core Team (2023). A Language and Environment for Statistical Computing_ (R Foundation for Statistical Computing). https://www.R-project.org/.

68. Zhou, F.Y., Weems, A., Gihana, G.M., Chen, B., Chang, B.-J., Driscoll, M., and Danuser, G. (2023). Surface-guided Computing to Analyze Subcellular Morphology and Membrane-Associated Signals in 3D. Preprint at Cold Spring Harbor Laboratory. https://doi.org/10.1101/2023.04.12.536640.

69. Vincent, A.E., White, K., Davey, T., Philips, J., Ogden, R.T., Lawless, C., Warren, C., Hall, M.G., Ng, Y.S., Falkous, G., et al. (2019). Quantitative 3D Mapping of the Human Skeletal Muscle Mitochondrial Network. Cell Rep. *26*, 996–1009.e4. https://doi.org/10.1016/J.CELREP.2019.01.010/ATTACHMENT/6774A23F-11B8-432E-8F6B-4FB14C8A91D1/MMC8.PDF.

Please cite this article in press as: Damianou et al., Integrative proximal-ubiquitomics profiling for deubiquitinase substrate discovery applied to USP30, Cell Chemical Biology (2025), https://doi.org/10.1016/j.chembiol.2025.04.004

CellPress
OPEN ACCESS

STAR★METHODS

KEY RESOURCES TABLE

REAGENT or RESOURCE	SOURCE	IDENTIFIER
Antibodies		
GAPDH (GAR1)	Invitrogen	CAT# MA5-15738
USP30	Atlas antibodies	CAT# HPA016952
USP30	MRC PPU	CAT# DU 36243
LETM1	Proteintech	CAT# 16024-1-AP
Tomm20 (D8T4N)	Cell signalling technology	CAT# 42406
Flag	Sigma Aldrich	CAT# F3040
β-actin (8H10D10)	Cell signalling technology	CAT# 3700
Anti-HA (12CA5)	Roche	CAT# 11666606001
Ubiquitin (FK1)	Sigma-Aldrich	CAT# 04-262
FKBP8	Proteintech	CAT# 11173-1-AP
S65 Phospho-ubiquitin	Cell signalling technology	CAT# 62802S
IgG Control (Rabbit-DA1E)	Cell signalling technology	CAT# 3900S
IRDye® 800CW Streptavidin	LICORbio	CAT# 926-32230
IRDye® 800CW Goat anti-Mouse IgG Secondary Antibody	LICORbio	CAT# 926-32210
IRDye® 800CW Donkey anti-Goat IgG Secondary Antibody	LICORbio	CAT# 926-32214
IRDye® 680CW Goat anti-Mouse IgG Secondary Antibody	LICORbio	CAT# 926-68070
IRDye® 800CW Goat anti-Rabbit IgG Secondary Antibody	LICORbio	CAT# 926-32211
IRDye® 680CW Goat anti-Rabbit IgG Secondary Antibody	LICORbio	CAT# 926-68071
Chemicals, peptides, and recombinant proteins		
DME Medium - high glucose	Sigma Aldrich	CAT# D6546
Fetal Bovine Serum (FBS)	Gibco	CAT# 10100147
GlutaMAX Supplement	Gibco	CAT# 35050061
Poly-D-Lysine	Gibco	CAT# A3890401
PhosSTOP phosphatase inhibitor	Roche	CAT# 4906837001
cOmpleteTM, Mini, EDTA-free Protease Inhibitor Cocktail	Roche	CAT# 11836170001
PierceTM DTT (Dithiothreitol)	ThermoFisher Scientific	CAT# 20290
Iodoacetamide	Sigma-Aldrich	CAT# A3221
Hydrogen peroxide (H_2O_2), 30% (wt/wt)	Sigma-Aldrich	CAT# H1009-100ML
Trifluoroacetic acid	Sigma-Aldrich	CAT# 91707
Formic acid	Sigma-Aldrich	CAT# 56302
Biotin-phenol	Sigma-Aldrich	CAT# SML2135
Sodium ascorbate	Sigma-Aldrich	CAT# A7631
Trolox	Sigma-Aldrich	CAT# 238813
Sodium azide	Sigma-Aldrich	CAT# S2002
Phosphoric acid	Sigma-Aldrich	CAT# 49685
SDS, 20% Solution, RNase-free	ThermoFisher Scientific	CAT# AM9820
RIPA Lysis and Extraction Buffer	Thermo Scientific	CAT# 89901
InstantBlue Coomassie Protein Stain (ISB1L)	Abcam	CAT# ab119211
L-Glutamine (200 mM)	Gibco	CAT# 25030149
Eagle's Minimum Essential Medium	Sigma	CAT# M2279

(*Continued on next page*)

Please cite this article in press as: Damianou et al., Integrative proximal-ubiquitomics profiling for deubiquitinase substrate discovery applied to USP30, Cell Chemical Biology (2025), https://doi.org/10.1016/j.chembiol.2025.04.004

Continued

REAGENT or RESOURCE	SOURCE	IDENTIFIER
Non-essential amino acids	Sigma	CAT# M7145
Ham's F12 Nutrient Mixture	Sigma	CAT# N4888
Lipofectamine 2000 Transfection Reagent	Invitrogen	CAT# 11668030
polybrene	Sigma Aldrich	CAT# TR-1003
blasticidin	Gibco	CAT# A1113903
Lipofectamine 3000 Transfection Reagent	Invitrogen	CAT# L3000001
RNAiMAX Transfection Reagent	Invitrogen	CAT# 13778150
compound **39**	Gift from Daryl S. Walter (Evotec)	CAS 2242582-40-5
HA-Ub-PA	This paper	N/A
Phosphate buffered saline (PBS)	Sigma Aldrich	CAT# D8537
Trizma base	Sigma Aldrich	CAT# T1503
Tris HCl	Roche	CAT# 10812846001
M_gCl_2	Sigma Aldrich	CAT# M2670
EDTA	Fisher Scientific	CAT# BP120-1
Sucrose	Alfa Aesar	CAT# A15583.36
HEPES	Sigma Aldrich	CAT# H4034
NaCl	Sigma Aldrich	CAT# S9888
Digitonin	Sigma Aldrich	CAT# D141
IGEPAL CA-630 (NP-40)	Sigma Aldrich	CAT# I3021
Carbonyl cyanide 3-chlorophenylhydrazone (CCCP)	Sigma Aldrich	CAT# C2759
DMSO	Alfa Aesar	CAT# 32434
Pierce™ High Capacity Streptavidin Agarose	Thermo Scientific	CAT# 20357
KCl	Sigma Aldrich	CAT# P9333
Na_2CO_3	Sigma Aldrich	CAT# 223530
Urea	Sigma Aldrich	CAT# U6504
Biotin	Sigma Aldrich	CAT# B4501
Glycerol	Sigma Aldrich	CAT# G2025
Triton-X-100	Sigma Aldrich	CAT# T9284
Bovine serum albumin (BSA)	Sigma Aldrich	CAT# A3059
Tween 20	Sigma Aldrich	CAT# P1379
Hoechst 33342	Invitrogen	CAT# H3570
IP lysis buffer	Pierce Thermo Scientific	CAT# 87787
N-Ethylmaleimide	Sigma Aldrich	CAT# E3876
MG132	Sigma Aldrich	CAT# M7449
Tandem Ubiquitin Binding Entity 1 (TUBE 1) Agarose	Life Sensors	CAT# UM401
MitoTracker® Red CMXRos	Cell signaling technology	CAT# 9082
16% Formaldehyde (w/v), Methanol-free	ThermoFisher Scientific	CAT# 28906
Critical commercial assays		
Duolink® *In Situ* Detection Reagents Orange	Sigma Aldrich	CAT# DUO92007
CyQUANT™ LDH Cytotoxicity Assay	Invitrogen	CAT# C20300
Pierce™ BCA Protein Assay Kit	ThermoFisher Scientific	CAT# 23225
PTMScan® HS Ubiquitin/SUMO Remnant Motif (K-ε-GG)	Cell signaling technology	CAT# 59322
Dynabeads™ Co-Immunoprecipitation Kit	ThermoFisher Scientific	CAT# 14321D
S-Trap™ micro	Protifi	CAT# C02-micro
S-Trap™ Midi	Protifi	CAT# C02-midi
MycoAlert detection kit	Lonza	CAT# LT07-318
Deposited data		
LC-MS/MS data	This paper - PRIDE	PXD054890
Uncropped Western blot	This paper - Mendeley Data	https://doi.org/10.17632/s7frkxwphg.1

(*Continued on next page*)

Please cite this article in press as: Damianou et al., Integrative proximal-ubiquitomics profiling for deubiquitinase substrate discovery applied to USP30, Cell Chemical Biology (2025), https://doi.org/10.1016/j.chembiol.2025.04.004

Continued

REAGENT or RESOURCE	SOURCE	IDENTIFIER
Experimental models: Cell lines		
HEK293	ATCC®	CAT# CRL-1573
HEK293T	ATCC®	CAT# CRL-3216
SH-SY5Y	ATCC®	CAT# CRL-2266
Oligonucleotides		
siRNA USP30	Dharmacon ON-TARGETplus SMARTpool	CAT# L-021294-00-0005
siRNA scrambled	Invitrogen	CAT# 4390844
Recombinant DNA		
pLenti-CMV-BsR-PGK-USP30-APEX-2	Vigene Biosciences	Custom made
Flag-HA-USP30	Addgene plasmid (wade harper)	CAT# 22578
pMD2G	Daniel Ebner Laboratory	Addgene plasmid # 12259
psPAX2	Daniel Ebner Laboratory	Addgene plasmid # 12260
Software and algorithms		
DIA-NN (1.8.1)	Steger et al.[39]	https://github.com/vdemichev/DiaNN
ImageJ	NIH	https://imagej.net/software/fiji/
Prism (Version 10.1.1 323)	Graphpad	https://www.graphpad.com/
Image studio lite (version 5.2.5)	LICORbio	https://www.licorbio.com/image-studio-lite
Perseus (version 1.6.15.0)	Tyanova et al.[59]	https://maxquant.net/perseus/
R (version 4.3.2)	R Core Team	https://cran.r-project.org
clusterProfiler package (version 4.10.1)[60]	Bioconductor	https://bioconductor.org/packages/clusterProfiler
Zen blue (version 3.10.103.01000)	ZEISS Microscopy	https://www.zeiss.com/microscopy/en/products/software/zeiss-zen.html
scikit-image (Python)	Van der Walt et al.[61]	https://scikit-image.org/

EXPERIMENTAL MODEL AND STUDY PARTICIPANT DETAILS

Cell culture

Cells were incubated at 37°C, 5% CO_2. HEK293 (*Homo sapien* female) cells were cultured in high glucose DMEM, supplemented with 10% FBS, and 2% L-glutamine. SH-SY5Y (*Homo sapien* female) cells were cultured in a 1:1 mix of Hams F12 nutrient Mix and EMEM, supplemented with 15% FBS, 1% Non-Essential amino acids and 2 mM Glutamax. Generally, Low-passage cells (fewer than 20 passages) were used throughout this study. Additionally, mycoplasma testing was performed routinely (MycoAlert detection kit), and cells were not maintained in culture for longer than 3 months.

METHOD DETAILS

Plasmid generation

The USP30-APEX2 was expressed using a pLenti-CMV-BsR-PGK-USP30-APEX-2 plasmid synthesized by Vigene Biosciences. APEX2 was conjugated to the C terminal of USP30, with a glycine/serine flexible linker. Flag-HA-USP30 was a gift from Wade Harper (Addgene plasmid # 22578; http://n2t.net/addgene:22578; RRID:Addgene_22578).[62]

Lentiviral packaging

HEK293T cells were plated in a T175 flask and incubated at 37°C with 5% CO_2 until they reached 85% confluency. The cells were then transfected with pMD2G, psPAX2, and the USP30-APEX2 plasmids using Lipofectamine 2000 according to the manufacturer's protocol. After two days of incubation, the supernatants were collected, filtered through a 0.45 μm filter, and subjected to ultracentrifugation to concentrate the viral particles.

Cell line generation

1.5×10^5 HEK293 cells were seeded in a 6-well plate and incubated overnight at 37°C and 5% CO_2. 24 hrs after seeding, USP30-APEX2 lentivirus with polybrene was added to the HEK293 cells at a concentration of 8 μg/ml and incubated overnight at 37°C

Please cite this article in press as: Damianou et al., Integrative proximal-ubiquitomics profiling for deubiquitinase substrate discovery applied to USP30, Cell Chemical Biology (2025), https://doi.org/10.1016/j.chembiol.2025.04.004

and 5% CO_2. 24 hrs after lentiviral treatment, the HEK293 cells were trypsinized and seeded into a 100mm dish (All cells were used). After 8 hours, 5 μg/ml blasticidin was added to both the negative control and the transduced cells. The cells were incubated for 10 days under selection, with the medium being replaced every 3 days.

Transient transfection

For DNA plasmid transfections, cells were seeded in 6-well plates and transfected for 24 hrs using Lipofectamine 3000 Transfection Reagent (L3000001, ThermoFisher UK) according to the manufacturer's instructions. The concentration of plasmids used can be found in the details of each specific experiment.

For siRNA transfection experiments, cells were grown in 6-well plates and transfected for 72 hrs with RNAiMAX Transfection Reagent (Invitrogen, 13778-150) following the manufacturer's protocol. A final concentration of 10 nM was used for the following Silencer Select siRNAs: control siRNA (4390844) and si-USP30 (Dharmacon ON-TARGETplus SMARTpool).

Compound 39 synthesis

'compound **39**' (Figure S1E), refers to CAS number 2242582-40-5. The inhibitor was >95% pure as assessed by HPLC analysis.[27]

HA-Ub-PA ABP labelling

Ubiquitin (Gly76del) with an N-term HA tag and C-term propargylamine (HA-Ub-PA) synthesis and lysate labelling was carried out as previously described.[26] HEK293 expressing USP30-APEX2 were treated with compound **39** for 6 hrs at the concentration indicated in the figure, washed 3 times in PBS and lysed in 50 mM Tris (pH 7.5), 5 mM $MgCl_2$, 0.5 mM EDTA, 250 mM sucrose and 1 mM DTT with bead beating. Lysates were then clarified at 600 *xg* for 10 minutes at 4°C and supernatant protein was quantified by BCA. HA-Ub-PA was then incubated with lysate protein (1:100 w/w) for 5 minutes at 37°C.

Membrane-cytoplasmic cellular fractionation

As previously described,[39] fresh HEK293 FRT cell pellets were resuspended in digitonin lysis buffer (50 mM Hepes, pH 7.5, 10 mg/ml digitonin, 150 mM NaCl) and incubated for 30 minutes at 4°C with continuous agitation. The sample was then centrifuged at 6,000 *xg* for 5 minutes at 4°C. The resulting supernatant, containing the cytoplasmic fraction, was carefully transferred to a new tube. The pellet was resuspended in a buffer containing 0.3% NP-40, 50 mM Hepes (pH 7.5), and 150 mM NaCl, and incubated on ice for 5 minutes. After centrifugation at 1,500g for 5 minutes, the supernatant, representing the membrane fraction, was collected into a separate tube and stored at −20°C until further analysis.

LDH release cytotoxicity assay

HEK293 cells expressing USP30-APEX2 were grown in a 96 well plate coated with Poly-D-Lysine. Cells were treated with 10 μM CCCP for 6 hrs and biotin-phenol for 30 minutes (N=3 wells) at the indicated concentrations. Cytotoxicity was measured as LDH release into the media using the CyQUANT™ LDH Cytotoxicity Assay (Invitrogen) according to the manufacturer's instructions. Briefly, 10 μl of lysis buffer per well (provided in the kit) for the maximal LDH activity controls, and 10 μl H_2O for all other samples was incubated at 37°C for 45 minutes with 5 % CO_2. After incubation 50 μl of media from each well was transferred to a new 96 well plate and 50 μl of reaction mixture was added to each well. Following a 30-minute room temperature incubation, 50 μl of stop solution was added to each well and the absorbance was measured at 490 nm and 680 nm. Biotin treated cytotoxicity was calculated as a percentage of the maximum LDH activity after subtraction of spontaneous control LDH activity.

Proximal ubiquitomics workflow - APEX2 proximity labelling

HEK293 cells expressing USP30-APEX2 were grown in T175 flasks coated with Poly-D-Lysine to 100% confluency, with 5 x T175 flasks pooled per condition. The medium was then replaced with fresh medium containing 10 μM CCCP, with either 5 μM of compound **39**, or DMSO as a control. The cells were incubated at 37°C and 5% CO_2 for 5.5 hours. Following this incubation, proximity labelling was performed as previously described.[36,49,63] Briefly, 2 μM phenol biotin was added to the media, and the cells were incubated for an additional 30 minutes. Subsequently, H_2O_2 at a concentration of 1 mM was added to the medium for exactly 1 minute. The cells were then washed four times with Quencher buffer (10 mM sodium ascorbate, 10 mM sodium azide, 5mM Trolox in DPBS), with each wash involving a 1-minute incubation.

The cells were lysed using lysis buffer (10 ml per 5 x T175 flasks) (RIPA lysis buffer containing 1 mM PMSF, 5 mM Trolox, 10 mM sodium azide, 10 mM sodium ascorbate, PhosSTOP phosphatase inhibitor and cOmplete Protease Inhibitor Cocktail) and centrifuged at 10,000 *xg* for 10 minutes at 4°C. At this stage 5% of lysate was taken for the 'labelled proteome' and processed for mass spectrometry analysis using the S-Trap™ micro digestion protocol according to the manufacturer's instructions, and the remaining lysate was incubated with 3.5 mL of streptavidin agarose beads for 1 hour at room temperature. The beads were then washed with 10 mL of the following buffers in the specified order: twice with RIPA buffer, then with KCl, Na_2CO_3, 2M Urea, 1% SDS and finally with 2 times with RIPA buffer.

Biotinylated proteins were eluted in 4 mL of 2x loading dye (100 mM Tris-HCL pH 6.8, 4% SDS, 20 % Glycerol) supplemented with 2 mM biotin and 20 mM DTT by boiling (98°C) for 10 min. Eluted material was subsequently processed for mass spectrometry analysis using the S-Trap™ midi digestion protocol according to the manufacturer's instructions. 10% of eluates from the S-Trap™ clean up were taken for LC-MS/MS analysis as the 'proximitome'.

Please cite this article in press as: Damianou et al., Integrative proximal-ubiquitomics profiling for deubiquitinase substrate discovery applied to USP30, Cell Chemical Biology (2025), https://doi.org/10.1016/j.chembiol.2025.04.004

Proximal ubiquitomics workflow - K-ε-GG immunoprecipitation

The subsequent K-ε-GG immunoprecipitation (IP) was performed according to the manufacturer's instructions with small differences. Briefly, lyophilized peptides were centrifuged for 5 minutes at 2000 x*g* at room temperature. To the dried peptides, 0.5 mL of 1X IAP bind buffer was added, and the peptides were resuspended mechanically by repeated pipetting. The solution was then centrifuged for 5 minutes at 10,000 x*g* at 4°C and transferred into a new Eppendorf tube.

For each sample, 10 μL of bead slurry was placed into a 1.5 mL Eppendorf tube. The beads were washed four times with 1 mL of ice-cold PBS. The soluble peptides were then transferred to the beads and incubated on an end-over-end rotator for 2 hours at 4°C. Afterwards, the samples were spun down at 2000 x*g* for 5 seconds to pellet the beads, placed on a magnetic rack for 10 seconds, and the unbound peptide solution was discarded.

The beads were washed with 1 mL of chilled HS IAP Wash Buffer (1X), resuspended, briefly centrifuged as before, placed on the magnetic rack for 10 seconds, and the wash buffer was removed. This washing step was repeated three additional times. The samples were then washed twice with 1 mL of chilled LCMS water. Ubiquitinated peptides were eluted by adding 50 μL of IAP Elution buffer and incubating at room temperature for 10 minutes with gentle mixing. The elution was repeated once more to ensure complete recovery of ubiquitinated peptides. Peptides were then purified by C18 and resuspended in 5% DMSO/5% FA for LC-MS/MS analysis.

The input material optimization shown in Figures 2G and 2H follow this USP30-APEX2 proximity labelling workflow with indicated number of 15 cm dishes as input.

Control proteome, control ubiquitome and labelled ubiquitome

HEK293 cells expressing USP30-APEX2 were grown in 10 cm dishes coated with Poly-D-Lysine to 100% confluency, with 1 x 10 cm dish used per condition. Cells were APEX2 labelled as detailed for the proximal-ubiquitome for the 'labelled ubiquitome'. Cells for the control proteome and control ubiquitome were not APEX2 labelled. Cells were treated with CCCP +/− compound **39**, lysed in 500 μL, clarified and processed using S-Trap™ midi as detailed for the proximal-ubiquitome. Where cells were not APEX2 labelled, 5% was removed for the control proteome. Remaining peptides were then K-ε-GG immunoprecipitated as detailed for the proximal-ubiquitome.

Liquid chromatography tandem mass spectrometry - LC-MS/MS

The proximal-ubiquitome was analysed on a timsTOF SCP (Bruker) LC-MS/MS system to maximise sensitivity. The input material optimization detailed in Figures 2G and 2H was analysed on an Orbitrap Fusion Lumos Tribid (Thermo) LC-MS/MS system. All other samples were analysed on an Orbitrap Ascend Tribid (Thermo) LC-MS/MS system.

APEX2 proximitome and total proteomics samples were analysed by LC-MS/MS using a Vanquish Neo UHPLC (Thermo) connected to a Thermo Orbitrap Ascend mass spectrometer (Thermo). The Vanquish Neo was operated in "Trap and Elute" mode using a PepMap Neo trap (185um, 300um x 5mm) and EASY-SPRAY PepMapNeo column (50cmx75um, 1500bar). Tryptic peptides were trap and separated using a 60 min linear gradient over 60 minutes (from 3 to 20% B in 40 min and from 20 to 35% in 20 min) at 300nl/min flow.

APEX proximitome and total proteomics samples were acquired in DIA mode with some slight changes from previously described method.[27,64] Briefly, survey scans (MS1) were acquired in the Orbitrap over the mass range of 350 – 1650m/z, with a 45k resolution, maximum injection time of 91 ms, an AGC set to 125% and a RF lens at 30%. MS2 scans were then collected using the tMSn scan function, with a 40 predefined variable width DIA scan windows[64] with a 30K orbitrap resolution, normalized AGC target of 1000%, maximum injection time set to auto and a 30 % collision energy.

K-ε-GG enriched ubiquitomics samples were analysed by LC-MS/MS using an Ultimate 3000 HPLC coupled to an Orbitrap Ascend Tribrid or an Orbitrap Fusion Lumos Tribid instrument (Thermo Fisher) using a nano-EASY spray source. Tryptic peptides were loaded onto an AcclaimPepMap100 trap column (100μm x 2cm, PN164750; ThermoFisher) and separated on a 50cm EasySpray column (ES903, ThermoFisher) using a 60 min linear gradient from 2 to 35% acetonitrile, 0.1% formic acid and at 250nl/min flow rate. Both trap and column were kept at 50C. Data were acquired in DIA-mode with 44 variable width windows optimised for GG workflows as previously described.[39] In brief, MS1 scans were acquired in the Orbitrap over the mass range of 350 – 1650m/z, with a 120k resolution, maximum injection time of 60ms, an AGC set to 300% and a RF lens at 30%. MS2 scans were then collected using the tMSn scan function, with a 44 predefined variable width DIA scan windows[39] with a 30K orbitrap resolution, normalized AGC target of 2000%, maximum injection time set to auto and HCD stepped collision energy set at 22, 27 and 30 %.

Proximal-ubiquitome samples were analysed using an Evosep One LC system (EvoSep) coupled to a timsTOF SCP mass spectrometer (Bruker) using the Whisper 40 samples per day method and a 75 μm x 150 mm C18 column with 1.7 μm particles and an integrated Captive Spray Emitter (IonOpticks). Buffer A was 0.1% formic acid in water, Buffer B was 0.1% formic acid in acetonitrile. Data was collected using diaPASEF[65] with 1 MS frame and 9 diaPASEF frames per cycle with an accumulation and ramp time of 100 ms, for a total cycle time of 1.07 seconds. The diaPASEF frames were separated into 3 ion mobility windows, in total covering the 400 – 1000 m/z mass range with 25 m/z-wide windows between an ion mobility range of 0.64–1.4 Vs/cm^2. The collision energy was ramped linearly over the ion mobility range, with 20 eV applied at 0.6 Vs/cm^2 to 59 eV at 1.6 Vs/cm^2.

Immunofluorescence/Proximity ligation assay

Cells were fixed with 4% paraformaldehyde at room temperature for 10 minutes, followed by three washes with PBS. Next, the cells were incubated with PBS containing 0.1% Triton-X-100 for 10 minutes at room temperature, followed by a PBS wash for 5 minutes.

Please cite this article in press as: Damianou et al., Integrative proximal-ubiquitomics profiling for deubiquitinase substrate discovery applied to USP30, Cell Chemical Biology (2025), https://doi.org/10.1016/j.chembiol.2025.04.004

Subsequently, the cells were blocked with 5% BSA in TBST containing 0.1% Tween 20 for 1 hour. Depending on the sample, the cells were then incubated with the following primary antibodies: ANTI-FLAG® M1 (1:1000) (Sigma Aldrich F3040), LETM1 (1:100) (Proteintech, 16024-1-AP), and TOMM20 (1:100) (Cell Signaling, 42406) at 4°C overnight. After primary antibody incubation, the cells were washed three times with TBST containing 0.1% Tween 20, incubating with the wash buffer for 5 minutes each time.

For the proximity ligation assay (PLA), the cells were incubated with PLA anti-mouse PLUS and anti-rabbit MINUS Duolink secondaries, followed by Duolink *In Situ* Orange Reagents, according to the manufacturer's protocol (Millipore Sigma).

For immunofluorescence, the cells were incubated with the secondary antibodies (Goat anti-Mouse IgG (H + L), Alexa Fluor 488-conjugated, and Goat anti-Rabbit IgG (H + L), Alexa Fluor 633-conjugated) in 1% BSA in TBST containing 0.1% Tween 20 for 1 hour at room temperature. The cells were then washed three times with TBST containing 0.1% Tween 20, incubating with the wash buffer for 5 minutes each time. For nuclear staining, the cells were incubated with Hoechst 33342 (1:1000) for 10 minutes at room temperature, followed by three washes with PBS.

Samples from both PLA and immunofluorescence were imaged using a high-content laser-based spinning disk confocal microscope (Opera Phenix Plus) with a 40x water objective. Images were collected and analyzed using Harmony® imaging and analysis software.

For colocalisation analysis, the images were processed using ImageJ, and Li's Intensity Correlation Quotient (ICQ) was calculated using the Coloc 2 plugin.

Immunoprecipitation

IP-Flag: Cells were washed twice with ice-cold PBS and then lysed in Pierce IP lysis buffer (25 mM Tris-HCl pH 7.4, 150 mM NaCl, 1% NP-40, 1 mM EDTA, 5% glycerol, PhosSTOP phosphatase inhibitor, and cOmplete Protease Inhibitor Cocktail). The lysates were incubated on ice for 10 minutes with periodic mixing and then clarified by centrifugation at 13,000 x*g* for 10 minutes at 4°C. The pre-cleared lysates were incubated with anti-FLAG M2 Magnetic Beads at 4°C for 4 hours. After washing three times with lysis buffer, the proteins bound to the anti-FLAG antibody were pulled down by 3X FLAG peptide elution buffer. Both the whole cell lysates and the pull-down samples were subjected to immunoblotting analysis.

IP-LETM1: Cells were washed twice with ice-cold PBS and then lysed in Pierce IP lysis buffer (25 mM Tris-HCl pH 7.4, 150 mM NaCl, 1% NP-40, 1 mM EDTA, 5% glycerol, PhosSTOP phosphatase inhibitor, and cOmplete Protease Inhibitor Cocktail). The lysates were incubated on ice for 10 minutes with periodic mixing and then clarified by centrifugation at 13,000 *xg* for 10 minutes at 4°C to remove cell debris. The pre-cleared lysates were incubated with anti-LETM1 antibody in a dilution of 1:100. The next day, lysates were incubated with 50uL of Dynabeads™ Protein G for Immunoprecipitation and incubated for 30 minutes at room temperature. After washing three times with lysis buffer, the proteins bound to the anti-LETM1 antibody were eluted by 2X Loading dye and 100mM DTT elution buffer. Both the whole cell lysates and the pull-down samples were subjected to immunoblotting analysis.

Tandem ubiquitin binding entity pulldown

HEK293 cells were grown in 150 mm dish to 100% confluency, with 1 x 150 mm dish per condition**.** The medium was then replaced with fresh medium containing 10 μM CCCP, with either 5 μM of compound **39**, or DMSO as a control. The cells were incubated at 37 °C and 5 % CO_2 for 6 hours. Cells were washed twice with ice-cold PBS and then lysed in Pierce IP lysis buffer (25 mM Tris-HCl pH 7.4, 150 mM NaCl, 1% NP-40, 1 mM EDTA, 5% glycerol, PhosSTOP phosphatase inhibitor, and cOmplete Protease Inhibitor Cocktail, 100mM N-Ethylmaleimide (NEM) and 10 μM MG132). The lysates were incubated on ice for 10 minutes with periodic mixing and then clarified by centrifugation at 13,000 g for 10 minutes at 4°C to remove cell debris. Supernatant was collected and 10% of sample was removed as "INPUT" for analysis by Western blotting. Endogenous ubiquitylated proteins were isolated from the soluble lysate at 4°C for 12 hrs using 50 μl of packed agarose TUBE (TUBE1, Life sensors, performed according to the manufacturer's instructions). Following four washes in TBST, bound proteins were eluted using reducing and denaturing SDS sample loading buffer and analysed by Western blot.

Lattice light sheet microscopy of mitochondria

For imaging mitochondria, 8-well glass-bottom IBIDI chambers were coated, and 5,000 cells were seeded on the surface. The next day, cells were transfected with 10 nM of either Silencer control siRNA or si-USP30, as described above. After 72 hours, cells were treated with DMSO or 10 μM CCCP for 6 hours. Thirty minutes before the end of the treatment, 100 nM MitoTracker® Red CMXRos (Cell Signaling, #9082) was added to the cells. Cells and the glass slides were washed and fixed in 1% PFA for 10 minutes before being washed and placed into PBS. Volumetric images of cells (using a 0.2μm step size) were taken using the Lattice Light sheet microscope 7 (LLSM7) from Zeiss using the 561nm laser at 5% power with 50ms of exposure.

QUANTIFICATION AND STATISTICAL ANALYSIS

The proximal-ubiquitome, proximitome, labelled proteome, normal proteome and normal ubiquitome were performed in technical quadruplicate (N=4), the labelled ubiquitome was performed in technical triplicate (N=3). Technical replicates refer to samples that were grown in separate cell culture flasks and processed separately throughout the experimentation.

Please cite this article in press as: Damianou et al., Integrative proximal-ubiquitomics profiling for deubiquitinase substrate discovery applied to USP30, Cell Chemical Biology (2025), https://doi.org/10.1016/j.chembiol.2025.04.004

LC-MS/MS data processing

All data were searched library-free with DIA-NN 1.8.1[39,66] with a Uniprot *Homo Sapiens* fasta (20,370 entries, retrieved on April 16, 2021). For ubiquitome searches all setting were left as default other than the addition of variable modifications (methionine oxidation, N-terminal acetylation and K-ε-GG ubiquitin remnant motif, with a maximum of 2 variable modifications allowed). Default search settings include 1 missed Trypsin/P cleavage, with fixed N-terminal methionine excision and fixed cysteine carbamidomethylation. For proteome and proximitome searches, settings were identical other than the K-ε-GG variable modification. Match-between runs was enabled for all searches, except for the input material optimization in Figures 2G and 2H.

LC-MS/MS data analysis

For ubiquitome data, peptide level information was extracted from the DIA-NN precursor matrix output. The output was filtered to remove any non-proteotypic identifications, collapsed to provide peptide level information by summing precursors with different charge states using R (version 4.3.2),[67] and filtered for the UniMod:121 K-ε-GG adduct. For proximitome and proteome data, the DIA-NN protein groups output matrix was used. All data was imported into Perseus (Version 1.6.15.0),[59] $\log_2$ transformed, filtered so that values were present in all replicates for at least 1 condition, median subtract normalised, and imputed using imputeLCMD k-nearest neighbour (KNN) with a neighbour number of 15. A Perseus two-sample students T-test with permutation-based FDR set to 5% was applied to extract significant changes as indicated in figures. Principle component analysis at Figures S2G–S2L was performed in Perseus (Version 1.6.15.0). Coefficients of variation at Figures S2A–S2F were calculated using Graphpad Prism (Version 10.1.1).

Permutation analysis of proximitome vs. proteome

Permutation analysis was carried out in R to establish the significance of the increased intensity of OMM proteins in the proximitome vs the proteome, when compared to all proteins and to those in the MM. This was achieved by multiplying the difference of each protein between the proximitome *vs* the proteome randomly by either +1 or −1 100000 times and then plotting the means of the differences as a distribution and comparing this to the mean difference of Mitocarta 3.0 annotated OMM proteins, MM proteins and to the proteins overall.

Gene set enrichment analysis of proximitome vs. proteome

Gene set enrichment analysis (GSEA) was performed in R[67] using the clusterProfiler package.[60] Genes were pre-ranked based on log2(fold change proximitome/proteome). Gene Ontology Cellular Component terms were interrogated against the pre-ranked gene list, providing normalised enrichment scores, leading edge signal scores, and p-values for each term. False discovery rate (FDR) was calculated using the Benjamini Hochberg (BH) Procedure. Gene sets with FDR < 0.05 were considered significantly enriched (as indicated in legends of Figure S4).

Image analysis of mitochondrial morphology using lattice light sheet microscopy

Images were deskewed and deconvolved using a constrained iterative algorithm (set to a level of 10) via the processing panel in Zen blue (version 3.10.103.01000). This gave an isotropic pixel value of 0.145. Mitochondria were segmented using a custom script that used a feathering algorithm to pick up on mitochondria outlines. This was in combination with multi-Otsu thresholding and a custom set of operators (i.e., erosions, closing, and filling of holes) from scikit-image (Python) to enable segmentation and separation of individual mitochondria.[61] Segmented objects <0.005 percentile and >0.995 percentile for mitochondrion surface area were excluded from further analysis, in order to reduced biases from segmentation artefacts. Separate organelles were given a unique identifier using the 'label' function from scikit-image. Segmented organelles had their geometric parameter measurements extracted (indicated in the table below) and standardized. Data was visualized with Uniform Manifold Approximation and Projection (UMAP). A gaussian kernal density estimate was plotted to produce the contour/density map of UMAP points for visualisation of mitochondria distribution shifts. Violin plots were used to show comparison between conditions for each metric listed below.

Metric analysed	Description
Surface area	Surface area was calculated by converting segmented mitochondria into a mesh[68] then using a custom script to extract the surface area from sum of the triangle faces (one side) that form the mesh.
Mito volume	Quantified by multiplying the number of pixels for each mitochondrion by the volume of a pixel.
Mito area/volume ratio	Mito area/volume
Mito complexity	Taken from Vincent et al., 2019.[69]
Mito sphericity	(Surface area *1.5)/
Mito compactness	(36*pi*volume)/(surface_area**2)
Mito roundness	(Surface area*pi*2/3)/6*volume**(2/3))
Euler number	Defined as N-H. N is the number of regions of the image (number of connected components of the object) and H is the number of holes in the image (isolated regions of the image's background).

Please cite this article in press as: Damianou et al., Integrative proximal-ubiquitomics profiling for deubiquitinase substrate discovery applied to USP30, Cell Chemical Biology (2025), https://doi.org/10.1016/j.chembiol.2025.04.004

ADDITIONAL RESOURCES

Uncropped Western blot images have been uploaded to Mendeley Data: https://doi.org/10.17632/s7frkxwphg.1 and are publicly available.